2007

Application of response surface methods to characterize missile performance

Angela Sheree Long

APPLICATION OF RESPONSE SURFACE METHODS TO CHARACTERIZE MISSILE PERFORMANCE

by

ANGELA SHEREE LONG

A THESIS

Submitted in partial fulfillment of the requirements
for the degree of Master of Science in Engineering
in
The Department of Mechanical and Aerospace Engineering
To
The School of Graduate Studies
of
The University of Alabama in Huntsville

HUNTSVILLE, ALABAMA

2007

In presenting this thesis in partial fulfillment of the requirements for a master's degree from The University of Alabama in Huntsville, I agree that the Library of this University shall make it freely available for inspection. I further agree that permission for extensive copying for scholarly purposes may be granted by my advisor or, in his/her absence, by the Chair of the Department of Mechanical and Aerospace Engineering or the Dean of the School of Graduate Studies. It is also understood that due recognition shall be given to me and to The University of Alabama in Huntsville in any scholarly use which may be made of any material in this thesis.

Angela Sherree Loy 3/13/07

(student signature) (date)

THESIS APPROVAL FORM

Submitted by Angela Sheree Long in partial fulfillment of the requirements for the degree of Master of Science in Engineering in Aerospace Engineering and accepted on behalf of the Faculty of the School of Graduate Studies by the thesis committee.

We, the undersigned members of the Graduate Faculty of The University of Alabama in Huntsville, certify that we have advised and/or supervised the candidate on the work described in this thesis. We further certify that we have reviewed the thesis manuscript and approve it in partial fulfillment of the requirements for the degree of Master of Science in Engineering in Aerospace Engineering.

3/13/07 (Date) D. Brian Landrum, Committee Chair

Hugh W. Coleman

Mark Tillman

Mark V. Bower 13MAR07 Mark Bower, MAE Department Chair

J. Auñón 3/14/07 Jorge Auñón, Dean of Engineering

Debra M. Moriarity 4/30/07 Debra Moriarity, Dean of Graduate Studies

ABSTRACT

The School of Graduate Studies
The University of Alabama in Huntsville

Degree Master of Science in Engineering **College/Dept** Engineering/ Mechanical and Aerospace Engineering

Name of Candidate Angela Sheree Long

Title Application of Response Surface Methods to Characterize Missile Performance

Response surface methods were applied to a computational missile model to investigate their ability to adequately predict simulation results, identify influential parameters, and decrease the amount of time needed for missile analysis. Three separate studies were conducted based on different input combinations of propellant mass flow rate, specific impulse, drag coefficient scale factor, pitch over rate gain, and launch elevation angle. A simulation matrix was designed for each study and executed to produce a polynomial response equation for the missile range. The residual range prediction errors of the response equation were computed over the range of input parameters. The response surface methods were found to adequately predict simulation results, identify the influential input parameters, and significantly reduce the analysis time.

Abstract Approval:

Committee Chair 3/13/07

Department Chair Frank V. Bower 3/14/07

Graduate Dean Debra M. Moriarty 4/30/07

ACKNOWLEDGMENTS

The work described in this thesis would not have been possible without the assistance of a number of people who deserve special attention. First, I would like to thank my research advisor, Dr. Brian Landrum, for his suggestion of this topic and his guidance throughout the stages of the work. Without his help, this work would not have been possible. I would also like to thank Dr. Hugh Coleman, Dr. James Swain, and Dr. Mark Tillman for their contributions to this study and dedication in the classroom. I would also like to acknowledge the help and encouragement that I received from my many colleagues and friends including Dr. Tony Gatlin, Mr. Sam Reaves, Dr. Alan Nicholson, Mr. Richard Toomey, and Dr. Brian Greiner. The encouragement received from each of these individuals helped me focus on the task at hand. Finally, I would like to thank my family and close friends for their encouragement and support during my entire graduate school experience. Without their support, I would not have continued to strive toward my goal of receiving an advanced degree.

TABLE OF CONTENTS

LIST OF FIGURES

LIST OF TABLES

LIST OF SYMBOLS

α	axial point location
α_{ISP}	ISP axial point location
a, b, c,d	main influence variable levels
A, B, C, D	main influence variables
Ae	exit area
$\beta, \beta_1, \beta_2, \beta_i$	response equation coefficients
β_0	response equation intercept
$\hat{B}$	coefficient matrix
βij	response equation interaction coefficient
C_A	axial force coefficient scale factor
C_{A0}	zero lift axial force coefficient
CCD	central composite design
CFD	computational fluid dynamics
C_N	normal force coefficient
g	gravitational acceleration
ISP	specific impulse
k	number of input variables
km	kilometers
kN	kilonewtons
μ	iterative eigenvalue for ridge analysis
MDOT, $\dot{m}$	mass flow rate
P_a	atmospheric pressure
RSM	response surface methodology
$s_{y(x)}$	standard prediction of error
X	coded simulation matrix
x_1, x_2, x_i, x_j	independent variables
x_s	stationary point
y	simulation response vector
$\hat{y}$	stationary point response

CHAPTER I

INTRODUCTION

Modeling and Simulation (M&S) is a well established and proven means of assessing the capabilities of a missile system. A common approach is to build a geometric model of the missile, simulate a matrix of flight conditions, analyze the flight characteristics, modify the matrix, and repeat the process. This approach often requires robust computing power for a significant length of time [1].

The level of complexity required for a missile simulation model depends on its final purpose. A simple system may only require a 3 Degree of Freedom (DoF) model to calculate the missile's ability to move through the x, y, and z coordinates. A 6 DoF model would be created for a much more complex missile when spatial coordinates and missile orientation (pitch, yaw, and roll) are very important [2]. Although a 6 DoF model is much more difficult to create, it often provides a better understanding of the actual missile flight performance in a real world scenario.

A number of parameters must be specified and calculated for a complete missile model. Physical characteristics such as length, diameter, nose shape and fin size must be defined to calculate aerodynamic coefficients through methods such as Missile DATCOM [3] or Computational Fluid Dynamics (CFD) [4]. The mass properties and

propulsion system must also be specified to calculate thrust profiles. All of these characteristics and calculations complete the weapon system model [2].

Upon completion of the model, input parameters such as mass flow rate, specific impulse, and axial force coefficient scale factor are varied for the execution of numerous Monte Carlo simulation runs to evaluate the flight characteristics for a given scenario. The execution of these simulations requires extensive computing power for considerable amounts of time [1]. A method is needed to shorten the time for the M&S process that also provides for response prediction and identification of influential parameters. The Response Surface Method (RSM) has the potential to decrease the amount of time needed for analysis and identify the most influential parameters while graphically representing the model's response.

The RSM encompasses a collection of statistical and mathematical techniques for developing, improving, and optimizing processes [5]. In a general RSM an analytic model is created using a single polynomial function to represent the relationship of the independent and dependant variables with the simulation. A least squares regression method is used to fit the mathematical equation to data from the experiment. This equation can be used to graphically represent the variable to response relationship and allow the analyst to determine a response at points not previously tested within the design space [6].

The Response Surface Methods were originally developed to aid in the understanding of the relationship between the varying parameters and response of an experiment [7]. By understanding these relationships, the amount of experimental data required to define a system is minimized. RSM techniques have been applied to a vast

range of experimental designs and empirical models. In 2002, Brown and Schamburg of the University of Virginia developed a modified version of RSM to include additional data mining techniques for complex simulation analysis [8]. Cioppa developed several experimental designs based on RSM methods and Latin hypercube designs to inspect twenty-two variables with only a few simulation runs [9].

The main objective of this thesis is to evaluate the capability of the RSM to adequately predict simulation results, identify influential parameters, and decrease the amount of time needed for missile system analysis. The example missile for this study is the German WWII era V2, also known as the Vengeance Weapon 2. The V2 was chosen because of the wealth of information readily available and for its similarities to many current missile systems. A generic missile computer model was built using the Matlab and Simulink software package and characteristic V2 related parameters were applied to represent missile flight performance. The construction of the model is explained further in Chapter IV.

Three separate RSM analyses using the V2 missile model were conducted. A single response equation was developed for each analysis to represent the missile simulation. The first analysis investigated accuracy of the polynomial response equation and the influence of four independent variables, (specific impulse, mass flow rate, pitchover gain, and axial force coefficient scale factor) and their interactions on the simulation. Two of the variables used in the first analysis are known to interact. In the second analysis specific impulse was held constant while focusing on the three remaining variables. The third analysis also considered the accuracy of the polynomial equation and the influence of three variables. Two of these variables, mass flow rate and axial force

coefficient scale factor, were the most influential parameters from the second analysis. A third variable, launcher elevation angle was added and the influence of this variable on the overall missile model performance was determined. Each of these analyses is examined in detail within Chapters V through VII.

CHAPTER II

RESPONSE SURFACE METHODOLOGY

The Response Surface Methodology (RSM) encompasses a collection of statistical and mathematical techniques useful for developing, improving, and optimizing processes [4]. RSM is used to define an approximate relationship between a performance measure, also known as the response, and a set of independent input variables associated with that response. The independent variables chosen for each analysis are subject to the control of the analyst.

A first or second order polynomial is typically used to represent the defined response surface of the process. The order of polynomial used depends primarily on the goals of the experimenter [10]. A first-order polynomial function of the form of

$$y = \beta_0 + \beta_1 x_1 + \beta_2 x_2 + \ldots + \beta_k x_k + \varepsilon \qquad (2.1)$$

is sufficient for investigating the system behavior around an area of minimal response curvature. A second order polynomial function of the form

$$y = \beta_0 + \sum_{i=1}^{k} \beta_i x_i + \sum_{i=1}^{k} \beta_i x_i^2 + \ldots + \sum_{i<j}^{k} \beta_{ij} x_i x_j + \varepsilon \qquad (2.2)$$

is useful when accurately representing the response surface around an area with greater curvature. Each of the equations represents a response with independent variables x_k, β_k coefficients, and $x_i x_j$ interactions where *k* is representative of the number of independent input variables with i and j representing the number of variable interactions. The second order polynomial function, Equation (2.2), was used for this study to represent the missile model response.

2.1 2^k Factorial Designs

To begin the RSM process, a design matrix must be created. This matrix is used to determine the variations of the input variables needed to accurately represent the response model. The RSM of this study utilized the 2^k factorial approach to create a design matrix based upon the number of k variables investigated. For instance, if k=3 independent variables are needed, the matrix would contain 2^3 or 8 varying simulation runs. Within the 2^k matrix each variable is considered to have a maximum and minimum value, represented as -1 or +1. This matrix with the representative maximum and minimum values is known as a coded variable matrix [7].

To properly execute the simulation runs of the 2^k coded matrix, the maximum and minimum variable combinations must be changed to realistic values, also identified as natural values. These values are predetermined by estimated and known system information. For example, the specific impulse of a missile might have a maximum

natural value of 211 seconds at a coded value of +1 and have a minimum natural value of 209 seconds at a coded value of -1. The engineer using the RSM process will make the final determination of the maximum and minimum values for each analysis.

Table 2.1 is representative of a typical 2^3 coded matrix. A, B, and C represent each independent variable while the trial numbers represent each simulation run. The labels are used to determine the influence of each independent variable and the variable interactions on the simulation. For example, label (1) identifies the trial or simulation run where all three independent variables are at their minimum values. Label *bc* represents the trial where the variable *A* is at its minimum value while the variables *B* and *C* are at their maximum values. The assigned labels are illustrated geometrically in Figure 2.1 as the corner points on a cube [11].

Table 2.1 Simulation Matrix for a 2^3 Factorial Design

		Independent Variables		
Trial	Label	*A*	*B*	*C*
1	(1)	-1	-1	-1
2	*a*	1	-1	-1
3	*b*	-1	1	-1
4	*ab*	1	1	-1
5	*c*	-1	-1	1
6	*ac*	1	-1	1
7	*bc*	-1	1	1
8	*abc*	1	1	1

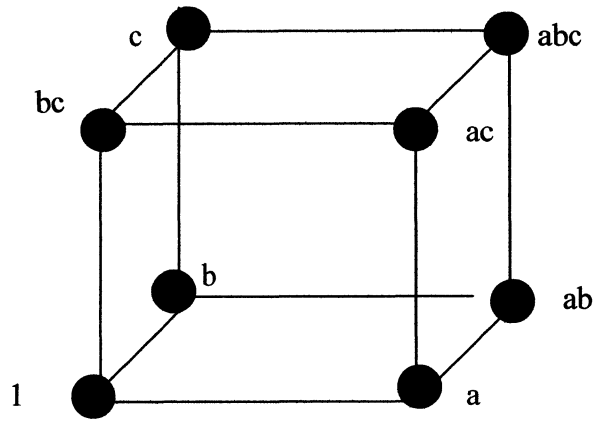

Figure 2.1 Geometric View of 2^3 Factorial Design

The influence of each variable and variable interaction is also known as the main effect. The main effect is the change in response caused by a change in level of the primary factors. For example, when variables *B* and *C* are at their minimum values, the effect of *A* is [*a*-(1)]/*n*. The variable *n* represents the number of replications for the experiment and *a* represents the resulting response for simulation number 2 (label a), when *A* is at its maximum value. Because this thesis is focused on computer simulations, the value for *n* is equal to one. The effect on *A* when *B* is at the maximum value and *C* is a minimum value is determined by [*ab-b*]/*n*. This process is carried throughout the design matrix until the average effect on *A* is determined using

$$A = \frac{1}{4n}[a + ab + ac + abc - (1) - b - c - bc]. \tag{2.3}$$

The main effects for each of the other variables are obtained using Eqs. (2.4) through (2.9). The variable with the largest effect is recognized as having the most impact on the simulations [5].

$$B = \frac{1}{4n}[b + ab + bc + abc - (1) - a - c - ac] \tag{2.4}$$

$$C = \frac{1}{4n}[c + ac + bc + abc - (1) - a - b - ab] \tag{2.5}$$

$$AB = \frac{1}{4n}[ab - a - b + (1) + abc - bc - ac + c] \tag{2.6}$$

$$AC = \frac{1}{4n}[(1) - a + b - ab - c + ac - bc + abc] \tag{2.7}$$

$$BC = \frac{1}{4n}[(1) + a - b - ab - c + ac + bc + abc] \tag{2.8}$$

$$ABC = \frac{1}{4n}[abc - bc - ac + c - ab + b + a - (1)] \tag{2.9}$$

Once the simulation results are recorded and the main effects of each variable determined, the response equation is calculated in the form of Equations (2.1) or (2.2). The β coefficients for the response equation are determined by

$$\beta = (X'X)^{-1}X'y, \tag{2.10}$$

where $\boldsymbol{X}$ is the n x p coded 2^k matrix inputs and y is the n x 1 vector of simulation results.

Once the polynomial response equation is developed, its accuracy must be verified. The accuracy is determined by placing the coded matrix values of +1, -1, and 0 in the equation and calculating the result. This result is then compared to that of the actual simulation result [12]. The number of k independent variables chosen for the experiment will have an effect on the accuracy of the equation. The greater the number of independent variables chosen for the analysis, the greater the amount of error in the resulting polynomial response equation [13].

2.2 Central Composite Design

The Central Composite Design (CCD) is often used to develop second order response equations due to its ability to provide information about the existence of curvature in the system [10]. In CCD, additional simulation runs are added to the 2^k factorial matrix to represent the face centered or axial points, and the center point within the cube. A typical CCD matrix is shown in Table 2.2.

Table 2.2 CCD Simulation Matrix

	Independent Variables		
Trial	*A*	*B*	*C*
1	-1	-1	-1
2	1	-1	-1
3	-1	1	-1
4	1	1	-1
5	-1	-1	1
6	1	-1	1
7	-1	1	1
8	1	1	1
9	-1.682	0	0
10	1.682	0	0
11	0	-1.682	0
12	0	1.682	0
13	0	0	-1.682
14	0	0	1.682
15	0	0	0

The center run provides information about the curvature of the system, the internal error estimation, and the estimation of quadratic terms in the system response equation. In the simulation run representing the center point, all of the values of the independent variables are nominal values. These nominal values are the average of the maximum and minimum values of each independent variable. In the coded matrix, the nominal values are represented as a value of zero. Figure 2.2 is a geometric representation of a CCD matrix.

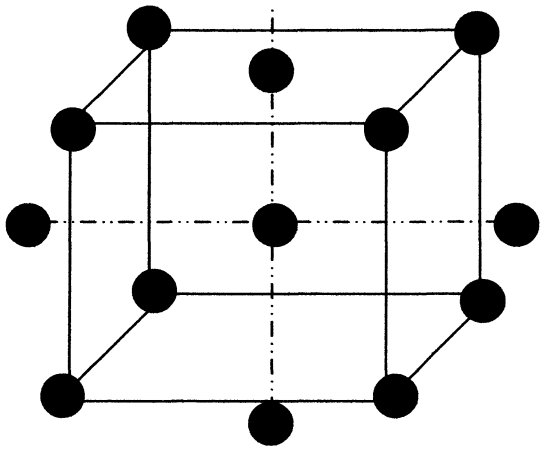

Figure 2.2 CCD Cube for k=3

The axial points of the matrix also contribute to the estimation of the quadratic terms of the system, but do not effect interaction terms within the system response equation [5]. For each simulation run representing an axial point, the axial distance from the center of the cube is chosen for one independent variable while the remaining variables stay at the assigned nominal values. The selection of the axial distance is very

important to providing good predictions throughout the region of interest [7]. The axial distance α for the coded matrix is calculated using

$$\alpha = \left(2^k\right)^{1/4}. \tag{2.11}$$

The natural value of α for the simulation runs is calculated by

$$\alpha_A = \left(\alpha * \frac{(\max(A) - \min(A))}{2}\right) + \left(\frac{(\max(A) + \min(A))}{2}\right). \tag{2.12}$$

2.3 Response Surface Plots

Two- and three-dimensional response surface plots are often used to explore RSM results. These response plots aide the analyst in determining the behavior of the response system relative to the different variables. By observing the plot shape and location, an analyst can verify if a maximum or minimum response for the system is achievable using the determined variables for the study. When achieving a maximum response at the center of the overall system is possible, a significant peak will be observed. If a noticeable valley is observed, a minimum value will be present at the center of the system. A saddle point is present when neither a peak nor valley is observed [14].

2.4 Stationary Point and Ridge Analysis

Another important aspect of a second-order system is the location of the center of the system also known as the stationary point. This stationary point represents one of three scenarios: a maximum response, a minimum response, or neither. In the case where

neither a maximum nor minimum response exists, the stationary point represents a saddle point. The stationary point can be determined by

$$x_s = -\frac{1}{2}\hat{B}^{-1}b. \tag{2.13}$$

The stationary point is a function of the fitted model and not of the true system itself. Each of the values for b is taken from the first order term coefficients in the fitted response Equation (2.2). The term $\hat{B}$ represents a matrix of the second order terms given by

$$\hat{B} = \begin{bmatrix} b_{11} & \frac{b_{12}}{2} & \frac{b_{13}}{2} & \frac{b_{14}}{2} \\ & b_{22} & \frac{b_{23}}{2} & \frac{b_{24}}{2} \\ Symm. & & b_{33} & \frac{b_{34}}{2} \\ & & & b_{44} \end{bmatrix}. \tag{2.14}$$

The predicted response of the system at the stationary point can also be calculated by

$$\hat{y}_s = b_0 + \frac{1}{2}x_s^{-1}b\ . \tag{2.15}$$

The type of response at the stationary point may be determined once the stationary point is calculated. The response type is first revealed by calculating the eigenvalues of the $\hat{B}$ matrix. If the corresponding eigenvalues are negative, the response is a maximum. Positive eigenvalues produce a minimum response. A mixture of both

positive and negative eigenvalues produces neither a maximum or minimum response. This result identifies the stationary point as a "saddle point." When a saddle point results from the stationary point calculations, the study may be stopped and a conclusion drawn that the stationary point does not lie within the specified analysis space. This would mean that the maximum or minimum response of the system resides outside the defined experimental region. In order to use the fitted model, only the independent variables assigned to form the fitted equation could be used. No other independent variable would be valid with the equation.

When a saddle point is defined for the system, ridge analysis can be performed to determine the nature of the system inside or on the perimeter of the experimental region [6]. Ridge analysis provides the ability to fix the stationary point of the system within a certain radius of interest. The stationary point along with the specified radius is then used to determine the maximum or minimum results obtained within that analysis space. By knowing the location of the maximum and minimum responses, one can choose a value for each variable to achieve a desired response. Ridge analysis is based on a method of steepest ascent for second order response surfaces.

To begin ridge analysis, we return to the fitted second-order response of Equation (2.2). In matrix form, the response equation is given as

$$\hat{y} = b_0 + x'b + x'\hat{B}x, \tag{2.16}$$

where b_0, b, and $\hat{B}$ are estimates of the intercept, linear, and second-order coefficients [5]. A constraint radius is placed around the experimental region to capture the system's behavior within that region. Using an iterative process, stationary points are calculated along the radius to maximize the system response within the experimental region. The

iterative process begins by assigning an initial eigenvalue to the variable μ and calculating the stationary points located along the radius by

$$(\hat{B} - \mu I)x = -\frac{1}{2}b. \tag{2.17}$$

The constraint radius for these stationary points is then calculated by

$$x'x = R^2. \tag{2.18}$$

This process is repeated until the desired constraint radius R is achieved [6]. The final stationary points for the constraint are then used to determine the maximum or minimum response along the assigned radius.

The determination of whether the response is either a maximum or minimum lies within the final value of μ and the eigenvalues for the matrix $\hat{B}$. When the value of μ exceeds the largest eigenvalue of $\hat{B}$, the stationary point will produce a maximum response on the constrained radius R. If the value of μ is smaller than the least eigenvalue of $\hat{B}$, the result will produce a minimum response on the constrained radius R [5].

A standard prediction error must be determined for each of the resulting response values lying along the constraint radii. The standard error is an estimate of the standard deviation of the predicted response over repeated experiments in which the same design and model are employed [5].

The standard error for the predicted responses lying along each radius is calculated by

$$s_{y(x)} = s\sqrt{x^{(m)'}(X'X)^{-1}x^{(m)}} \,. \tag{2.19}$$

The variable s is the standard deviation of the response values while X is the original coded matrix and $x^{(m)}$ is the particular variable location of response along the radius.

CHAPTER III

VENGEANCE WEAPON 2 HISTORY AND ENGINEERING

The Vengeance Weapon 2 (V2) was the example missile chosen for this analysis due to the wealth of technical information available and its similarities to missile systems of today. From the ogive nose and symmetric body to the graphite rudders and large fins, many missiles of today are patterned from the V2.

The V2 was the first short range ballistic missile to be used in warfare during World War II. Developed by a team of German scientists led by Dr. Werner von Braun and General Walter Dornberger, the V2 became the role model of rocketry for the world [15]. Although the accuracy of the missile was questionable and it wasn't deployed until late in the war, it sparked the interest of many governments [16]. This truly began the development of the ballistic missiles we know today.

3.1 History of the V2

With the publishing of articles by Hermann Oberth in Germany and Robert Goddard in the United States, the fascination with rocketry soared [15]. The German Army Ordinance (GAO) office even took an interest in rocketry of the future. This interest wasn't for space travel, but for delivering deadly weapons to an enemy during wartime. The Treaty of Versailles ending World War I made no mention of rockets;

therefore, the GAO office saw rocket development as a legal pursuit under the terms of the settlement [16]. In December 1930, GAO officers agreed to pursue the developments of rockets as weapons and appointed Major General Walter Dornberger to head the project.

Soon after the meeting, Dornberger set out to develop a rocket to meet the needs of the GAO. He began by looking to commercial industry for a rocket design. In April 1932, Rudolf Nebel and his assistants, Hermman Oberth, Klaus Riedel, and Wernher von Braun, were invited to make a secret demonstration of their latest rocket project. Although the rocket failed to impress the Ordinance office, the abilities of one of the young scientists did catch their eye. The GAO was so impressed with Werner von Braun that they offered him a job working on the missile program. He reported for work in December of the same year.

Missile design, testing, and development began soon after von Braun's employment. By 1933, von Braun set out to accomplish three major objectives. His first objective was to develop engines based on various aluminum alloys. Using lightweight aluminum would help increase the overall performance of the missile. The second objective was also related to the propulsion of the missile. Von Braun wanted to fully automate the ignition and tank pressure operations. Coordinating the exact timing for the release of the oxidizer and fuel with ignition was crucial for the success of the program and the safety of all involved with it. The last objective was simply to design and construct the missile. By June 1933 a design for the first missile was complete [17].

The first missile was known as the Aggregate-1 (A-1). The German scientists knew that the propellant used for the 2.9 kN thrust motor was not stable enough for a

missile to spin on its axis like an artillery shell. To temporarily correct this problem, the nose cone of the A-1 was designed to be a large gyroscope for stabilization of the missile. The nose would be spun up to 9,000 rpm before launch and ran on its momentum during flight. Due to many mechanical failures, the A-1 never flew [15].

By December 1934 the next missile, Aggregate-2 (A-2), was complete and ready for flight. The main difference between the A-1 and the A-2 was that the gyroscope was located between the fuel and oxygen tanks on the A-2. This position was closer to the missile's center of gravity. The first flight of the A-2 was a success, with the missile reaching an altitude of 1,700 meters. This was the first step for the GAO to prove that it was feasible to produce a ballistic missile that could have a very long range.

The Aggregate-3 (A-3) was much larger than the A-1 and A-2. The missile was 6.5 meters long with a 14.7 kN thrust motor and weighed 73.4 kN at launch. A more complicated gyroscope control system was designed for the A-3. Each gyroscope was coupled with exhaust vanes to direct the missile's course. Nearing the end of 1937, the A-3 was ready for flight. For the first five seconds of flight, the missile seemed to perform quite well. Soon after that time it began to arc over and tumble uncontrollably. Each A-3 tested resulted in similar failures. An investigation concluded that the guidance system designed for the A-3 could not control such a massive body [15].

The design process for the next missile began during the construction of the A-3. Due to the unsuccessful flights of the A-3, the planning for the Aggregate 4 (A-4) was temporarily put on hold. Another test missile was planned to ensure better results before the final missile would be produced.

This test missile, Aggregate 5 (A-5), was built much like the A-3. It was about the same size and used the same propulsion system. The guidance system was redesigned and the jet vanes were made of graphite instead of molybdenum [15]. The A-5 successfully flew many times, giving the scientists the confidence to continue the final missile design.

The engineers and scientists developing the A-4 faced an enormous technological challenge. The new missile would need to fly at five times the speed of sound and be guided to targets approximately 300 kilometers away. The missile engine would also have to be seventeen times more powerful than the largest motor constructed. To conquer these obstacles, Dornberger felt that in-house research and working technological capability would provide a more efficient way of developing the A-4. This concept proved to be a success. The first successful test of the A-4 occurred in October of 1942. In only five years, the key technologies needed to ensure the success of the guided missile were mastered: a large liquid fuel engine, supersonic aerodynamics, and practical guidance and control. Although many problems still existed with the A-4, the German Army Ordinançe group insisted that the missile be made ready for production. On December 31, 1943 the first four production A-4 missiles rolled off the line while tests and planning continued. On August 29, 1944 Hitler demanded that the A-4, now known as the Vengeance Weapon 2, be deployed immediately. The long awaited V2 had entered the war.

3.2 V2 Engineering and Performance Characteristics

The 14 meter long V2 missile launched with a total mass of 13,000 kilograms, including a 1000 kg warhead. The missile was fueled with a combination of ethyl alcohol, water, and liquid oxygen. A detailed drawing of the V2 engine is given in Figure 3.1. A steam turbine, operating on a mixture of hydrogen peroxide and sodium permanganate, produced the power for two rotary pumps to deliver the fuels to the combustion chambers [18]. A small chamber located above the combustion chamber housed injection nozzles for the fuel and oxidizer. This improved the mixing process and atomization of the two propellants prior to burning. The spherical-shaped combustion chamber contained four rings of holes used to slowly seep alcohol into the chamber. This acted as an internal insulator to cool the chamber from the massive heat flux produced by the burning gases. Regenerative cooling (fuel circulating within the engine cooling jacket) was also used to absorb the excess heat. The propulsion system produced approximately 252 kN of thrust at liftoff and increased to a maximum of 712 kN during flight [17].

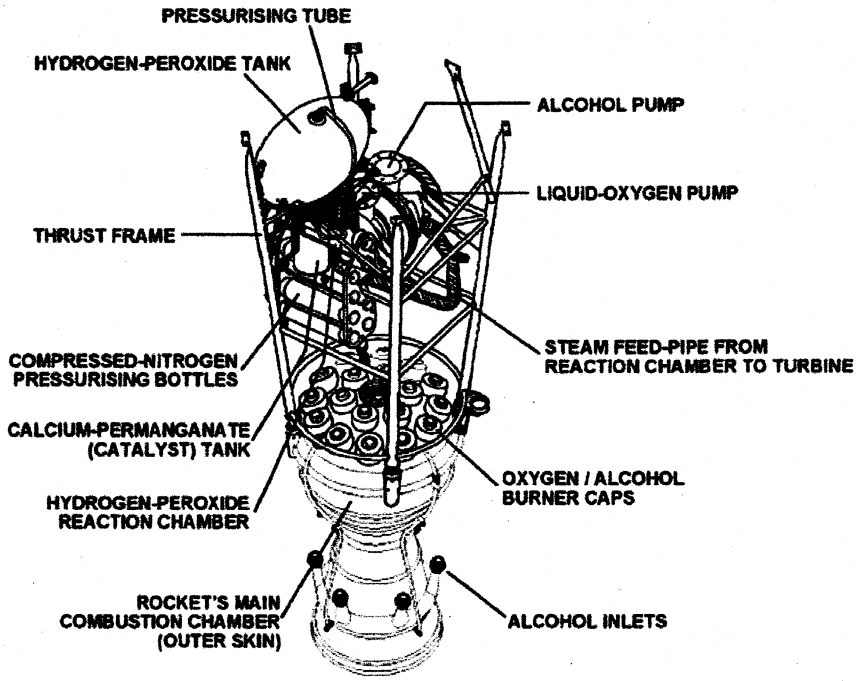

Figure 3.1 V2 Engine [17]

The missile was guided during engine burn by two gyroscopes connected to four graphite rudders and four jet vanes. The jet vanes were located inside the nozzle bell allowing them to deflect the exhaust, thus causing the missile to rotate in the direction needed. The vertical gyroscope sent a signal to the vanes and rudders in the vertical direction to control pitch, while the horizontal gyroscope sent a signal to the jet vanes and rudders in the horizontal direction to control yaw and roll stabilization. Beginning four seconds into flight, the horizontal gyroscope would send signals to direct the missile to an angle of 45 degrees over a period of 43 seconds. The fuel supply was shut off once the missile gained enough velocity to reach the target. This was done by one of two methods. The first method consisted of an on board device that would determine when the needed velocity was achieved and would send a signal for engine shut down. The

second and most accurate method was to terminate the thrust from the ground via a radio signal. Once the missile engine was shut down, the missile acted as a ballistic artillery shell during the remainder of the flight [15].

The body of the V2 missile was shaped much like a rifle bullet and constructed with a thin skin of sheet metal supported by circular and longitudinal ribs. Four large swept fins with an approximate span of 3.6 meters were attached to the boattail to stabilize the missile during launch and flight. The internal layout of the missile is shown in Figure 3.2 and the outer body of the missile is shown in Figure 3.3.

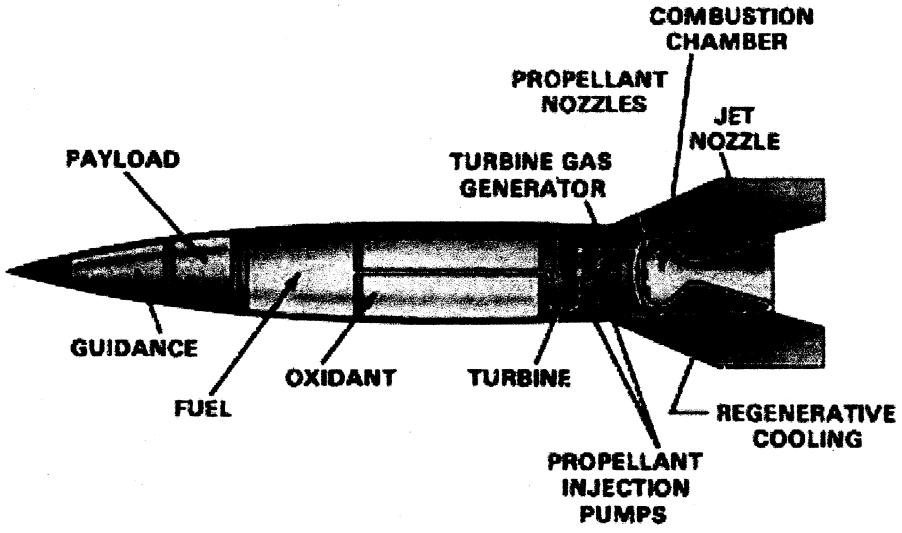

Figure 3.2: Internal Layout of the V2 Missile [17]

Table 3.1 lists the performance characteristics of the V2. The missile had a maximum range of 300 km and a maximum altitude of 80 km. The entire flight of the missile lasted for approximately 320 seconds with engine shut off occurring 63 seconds into flight at an altitude of 28 km. A 1000 kg warhead traveled the duration of the flight and detonated upon impact.

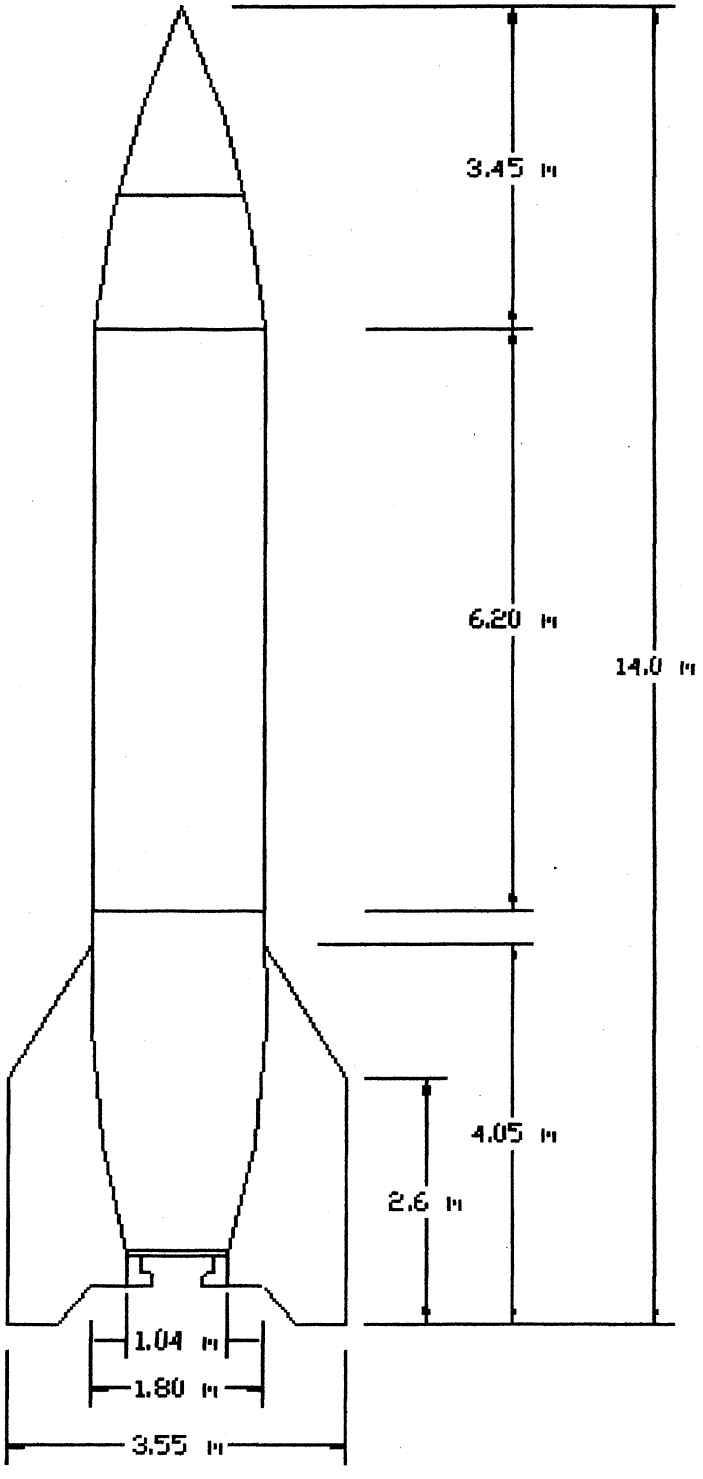

Figure 3.3 V2 Schematic

Table 3.1 V2 Performance Characteristics

Missile Length	14 m
Body Diameter	1.65 m
Fin Span	3.56 m
Missile Mass	13,000 kg
Warhead Mass	1000 kg
Thrust_Liftoff	244.7 kN
Burn Time	65 sec.
Exhaust Velocity	2000 m/s
Burnout Velocity	1500 m/s
Isp	215 sec.
Maximum Range	300 km
Maximum Altitude	80 km
Flight Time	320 sec.

The warhead for the V2 needed to be very powerful and stable during flight. Amatol, a combination of 60 percent TNT and 40 percent ammonium nitrate, was chosen. This type of explosive was known to be very powerful with very little sensitivity to shock and heat. The detonation fuses were located in the nose and at the base of the warhead. Each fuse contained a small primer charge that initiated the detonator. The detonator, Penthrite, was housed in a 3.5 centimeter tube that ran along the axis of the warhead and was connected to the fuses at each end. During impact, the fuses detonated the primer, which set off the detonator, causing the main charge to then explode [15].

Through many years of trials and hard work, the German scientists and engineers were successful at developing the first known short range ballistic missile. Although the missile was not known for its accuracy, it was recognized for the breakthroughs in technology that led to the ballistic missile capabilities that exist today.

CHAPTER IV

THREE DEGREE OF FREEDOM MISSILE MODEL

A three degree of freedom, (3 DoF) generic missile model was built with the commercial MATLAB/Simulink software. The purpose of this model is to represent all the known characteristics of a missile and simulate an actual flight. Two main modules comprise the model: the environment and the missile.

4.1 The Environment Module

The Environment module represents the Earth and atmospheric conditions within which the missile flies. Standard atmospheric data tables provide air density, pressure, and speed of sound during the missile simulation. As the altitude of the missile is calculated, the corresponding atmospheric conditions are extracted from the tables and sent to various modules within the global model. These atmospheric conditions are then used to determine the location and various properties of the missile during flight.

Stop flags are included within the Environment module of the missile model to allow the simulation to stop if an error ever occurs. These stop conditions use the time of flight and missile position to determine the appropriate time for the simulation to end.

Three earth models are also included within the Environment module. These are the flat earth, round earth, and WGS-84 models [2]. Each earth model uses reference

positions such as latitude, longitude, altitude, and earth radius to calculate the different coordinate systems within which the missile would fly. The round earth model was used for this project.

4.2 The Missile Module

The guidance, propulsion, and aerodynamics models encompass the most significant components within the Missile module. Each of the models was designed using technical characteristics of a generic missile system. Input blocks were utilized throughout the model to adapt it to any type of missile system needed. In the case of this project, known characteristic values of the V2 were applied using input blocks.

Guidance is the logic that issues steering commands to the vehicle to accomplish flight objectives [2]. The generic missile module uses a simple flight path guidance scheme to replicate the guidance of the missile during flight. As shown in the Guidance Model schematic, Figure 4.1, the pitch rate of the missile during flight is calculated by subtracting the current flight path angle from the known final flight path angle and applying a pitchover gain to increase or decrease the amount of pitch achieved at a given time. The pitch rate is not activated until the time of flight has exceeded the specified pitchover start time. The normal acceleration of the missile is then calculated by multiplying the determined pitch rate times the magnitude of the missile's velocity. The values of both the normal acceleration and pitch rate of the missile during flight are passed back into the equations of motion and aerodynamics modules to update the missile state during flight [19].

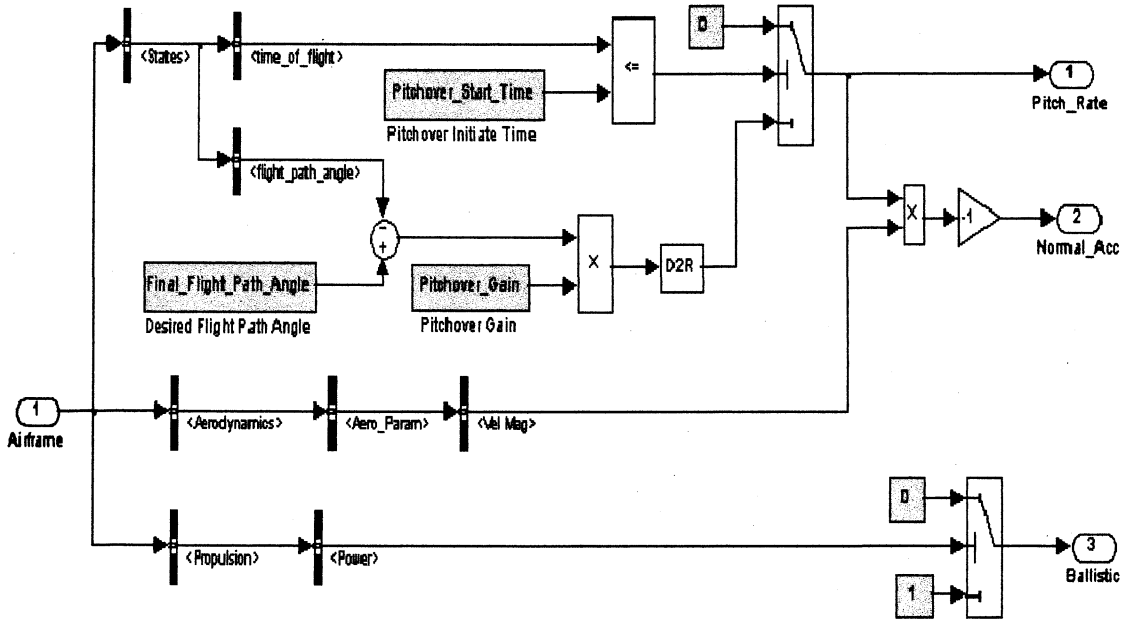

Figure 4.1 Flight Path Guidance Module

The propulsion model located within the missile module contains the calculations needed to determine instantaneous mass and thrust of the missile during flight. This model was built using basic principles of rocket propulsion. Missile characteristics such as mass flow rate, specific impulse (ISP), and nozzle exit area are required to complete propulsion calculations for the model. Specific impulse is a ratio of thrust to propellant flow rate. The mass flow rate ($\dot{m}$) is the amount of propellant expelled during the flight [20].

As revealed in the Propulsion Model schematic, Figure 4.2, the known mass flow rate of the propellant is integrated to determine the amount of mass burned at each specific time interval. This burned off mass is then subtracted from the initial mass to predict the remaining missile mass during flight. Once the engine shuts down, the remaining mass consists of only the body, warhead, and any guidance components.

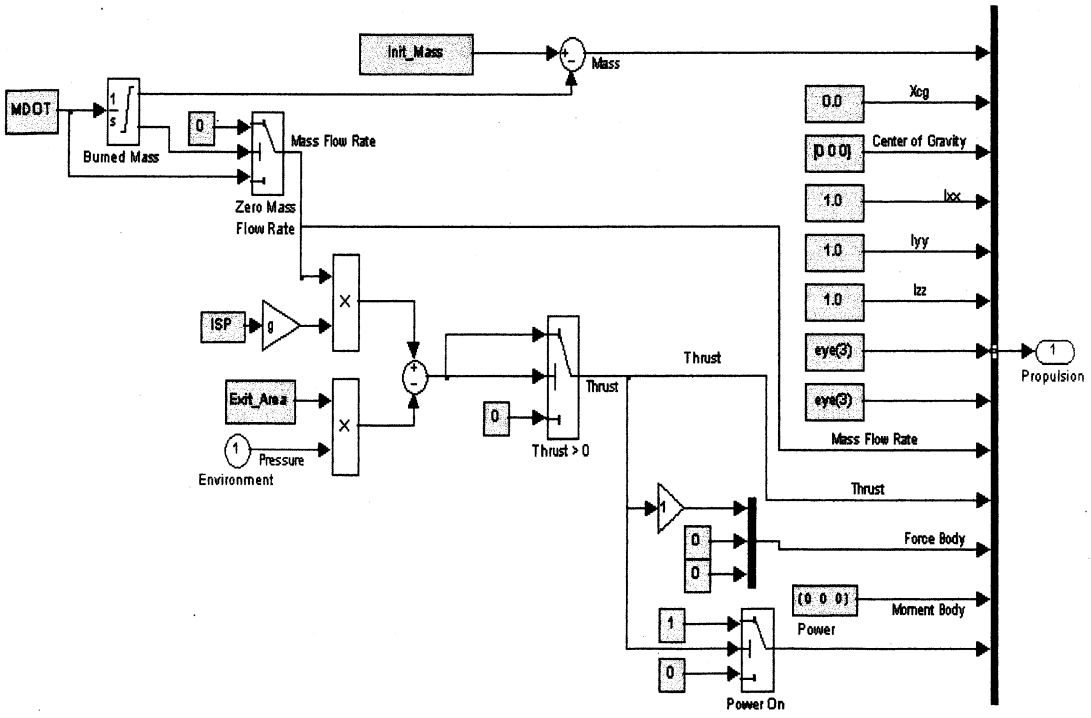

Figure 4.2 Propulsion Model

The thrust of the missile during engine burn is also calculated within the propulsion model of the missile module by

$$Thrust = ISP * \dot{m} * g - A_e * P_a, \tag{4.1}$$

based on the approximate ISP, mass flow rate ($\dot{m}$), gravitational acceleration, atmospheric pressure (Pa), and known nozzle exit area (Ae). The resulting thrust and mass properties from the propulsion model are passed on to the aerodynamics and equations of motion modules to calculate velocity, acceleration, and position of the missile during flight.

Determining the aerodynamic properties for a missile is often a more complicated process than that of the guidance or propulsion. Geometric characteristics of the missile body such as length, diameter, nose shape, and fin size must be specified in order to predict the aerodynamic coefficients for that body. Common methods to obtain the aerodynamic properties of a missile include semi-empirical methods such as Missile DATCOM [3] and AeroPredictor code (AP02) [4] or numerical prediction by Computational Fluid Dynamics (CFD) codes [21].

The actual flight envelope of missiles is comprised of viscous flow phenomenon and viscous CFD codes are computationally intensive. Therefore, inviscid Euler codes coupled with semi-empirical methods are often used to adjust the inviscid CFD results for the effects of viscous skin friction and base drag. This method is widely used for production purposes because it is accurate enough for most applications and can be obtained for reasonable cost in reasonable time [21]. The method chosen for the aerodynamic analysis depends primarily on the amount of information known about the missile and time frame required to conduct the analysis.

The generic aerodynamics model located within the missile module is designed for ease of operation. Aerodynamic property data, obtained from one of the analytical or computational methods mentioned above, is placed in table format and linked to the atmospheric properties from the Environment module. Calculated altitude and Mach number values from the Environment module are then used to access the needed normal force coefficients (C_N) and the axial force coefficients (C_A) of the missile during flight. The schematic of the generic aerodynamics coefficients model is shown in Figure 4.3.

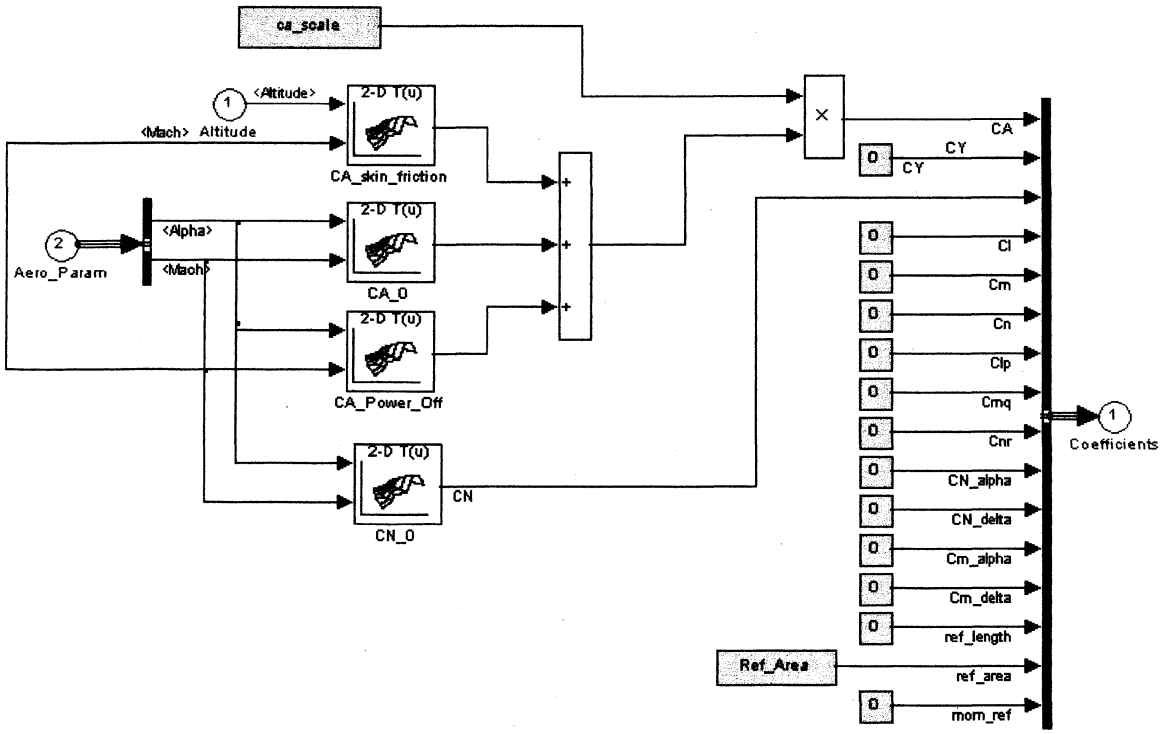

Figure 4.3 Aerodynamic Coefficients Model

4.3 Application of V2 Characteristics to the Generic Missile Model

The WWII era V2 missile was chosen for this study because of the wealth of information available and the similarities it holds to missiles of today. The V2 is known as the first short range ballistic missile. The missile is launched vertically and begins a 45 degree pitch four seconds into flight. The maneuver is completed within 43 seconds of flight and remains guided at this angle until engine shut down. The missile then flies in a ballistic trajectory until impact [16]. The known V2 guidance characteristics such as the final flight path angle, pitchover start time, and an approximate pitchover gain were input into the generic guidance model. The guidance model behaved in an expected manner and the missile flew with the angles specified. Figure 4.4 is a plot of the simulated V2 trajectory.

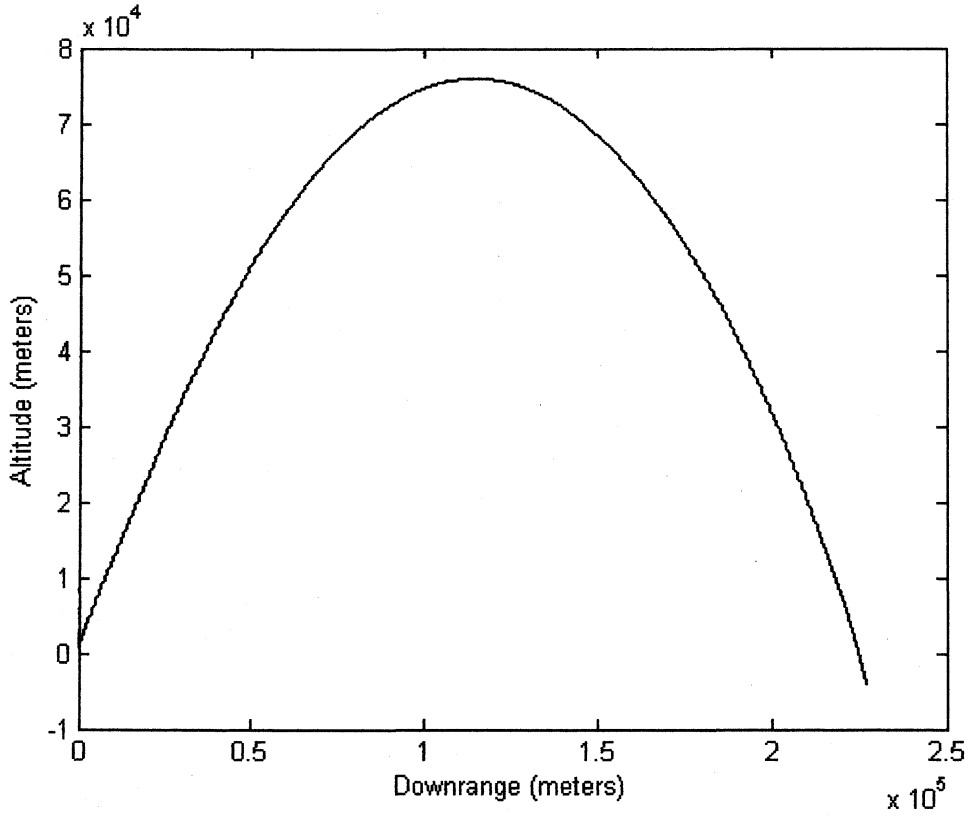

Figure 4.4 Simulated V2 Missile Trajectory

The V2 is a liquid bi-propellant system. This means that the engine thrust is a result of the combustion between a fuel and oxidizer. In the case of the V2, liquid oxygen serves as the oxidizer and 75% ethyl alcohol is the fuel. This fuel-oxidizer combination typically produces a sea level ISP of 239 seconds. Due to inefficiencies of the engine, the nominal ISP of the V2 is estimated to be 210 seconds [18].

The approximate burn time of the engine is 68 seconds. The approximate mass flow rate is calculated by dividing the total propellant mass by the engine burn time. The mass flow rate of the missile during flight can vary due to amount of actual fuel expelled. For example, to achieve a shorter downrange, only a small amount of fuel may be burned during flight. In the case of maximum downrange, the entire mass of fuel will be burned.

For this simulation, it is assumed that a maximum downrange is achieved and the total fuel mass is burned. The approximate values of ISP and mass flow rate are used as inputs for the generic propulsion model to determine the thrust and remaining mass of the V2 during flight. Equation (4.1) is used to calculate the thrust of the missile during flight. As the missile increases in altitude atmospheric pressure decreases producing a thrust profile as shown in Figure 4.5. Since the mass flow rate of the missile is assumed constant during flight, a linear mass decrease is produced. The missile mass profile is shown in Figure 4.6.

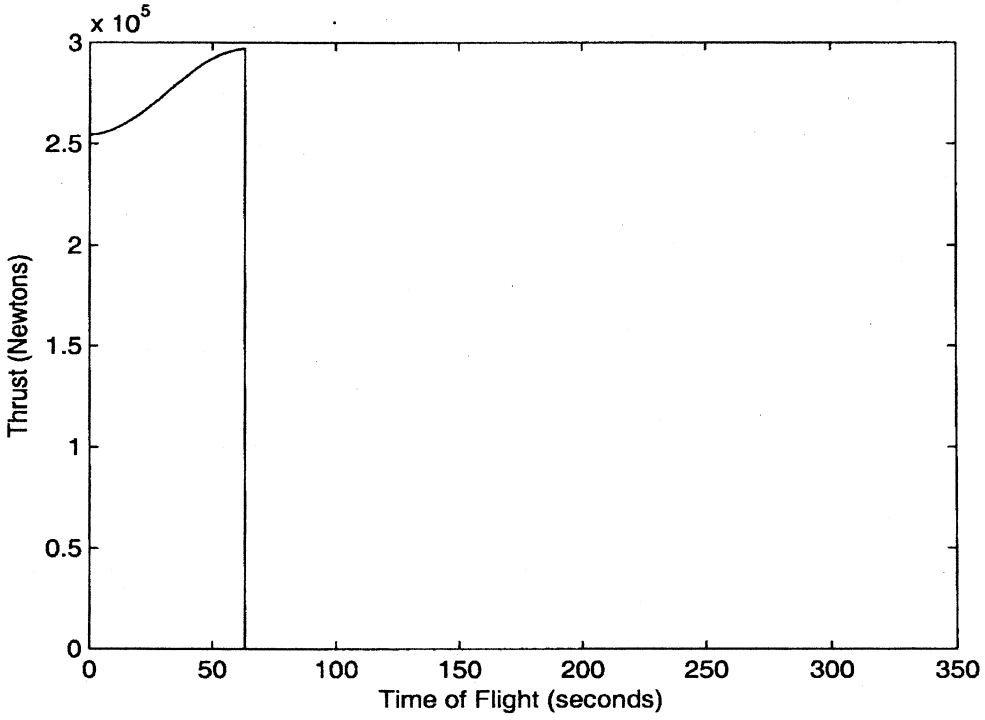

Figure 4.5 Missile Thrust Profile

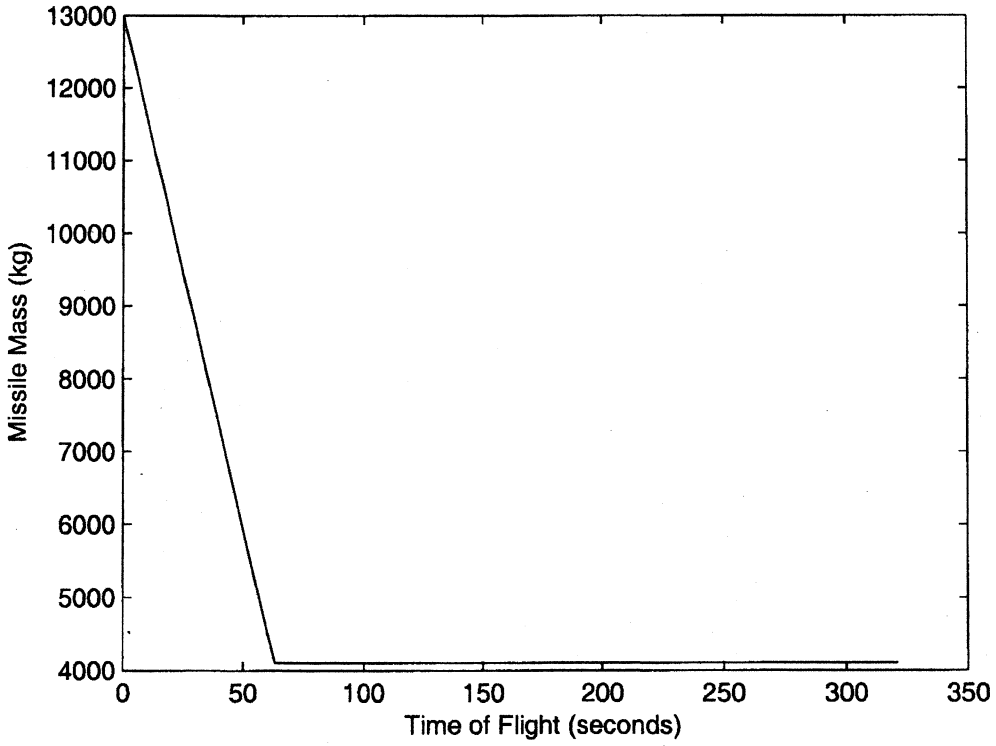

Figure 4.6 Missile Mass During Flight

Replicating the aerodynamics of the V2 was a more complicated process than was the guidance or propulsion systems. Detailed drawings were available through various sources, but no aerodynamic data was accessible. Although Missile DATCOM [3] and CFD methods were both used to predict the aerodynamic coefficients for the V2, only CFD predictions were used in this study.

A three-dimensional solid watertight model of the V2 was created and a Cartesian grid of approximately one million cells was generated around the body of the missile. A modified Tiger flow solver that calculates the inviscid flow of a compressible fluid while adjusting for the boundary layer and base pressure was used to properly predict drag

forces along the body [22]. This solver utilizes Jameson's four-stage Runge-Kutta time stepping algorithm with central differencing to solve the flow properties within the determined control volume [23]. Table 4.1 shows the simulation run matrix of nine mach numbers, six angles of attack, and five altitudes used to build a basis for the aerodynamic analysis. Figures 4.7 and 4.8 graphically present the anticipated axial (C_{AO}) and normal (C_N) force coefficients determined through the CFD analysis.

Table 4.1 Aerodynamic Input Matrix

MACH	ANGLE OF ATTACK (DEGREES)	ALTITUDE (METERS)
0.5	0	0
0.7	2	5000
0.9	4	10000
1.1	6	20000
1.3	8	30000
1.5	10	
2.0		
3.0		
5.0		

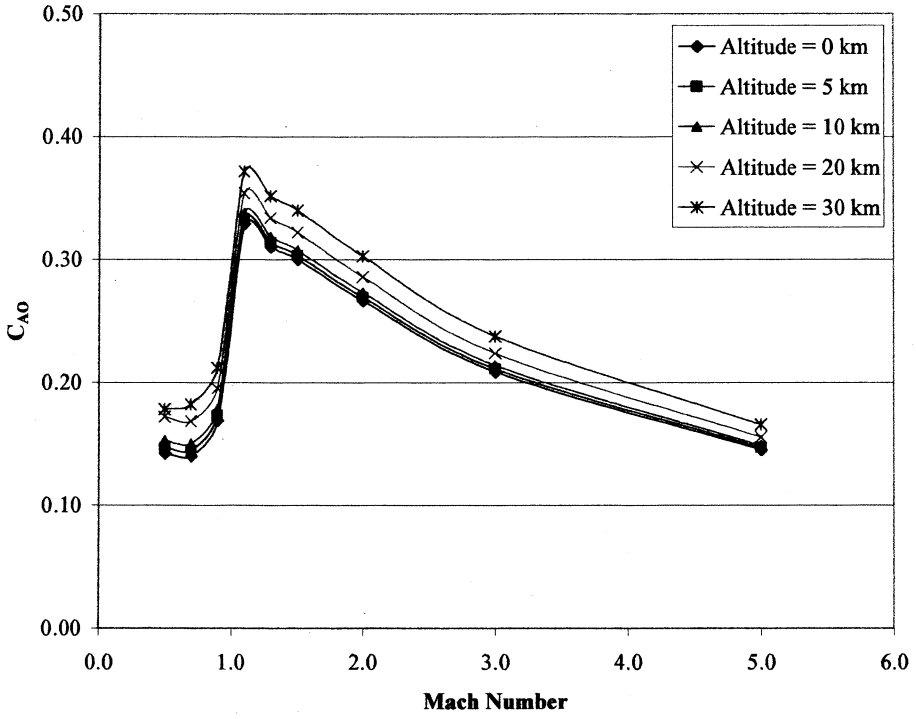

Figure 4.7 Axial Force Coefficients Calculated by Tiger CFD Code

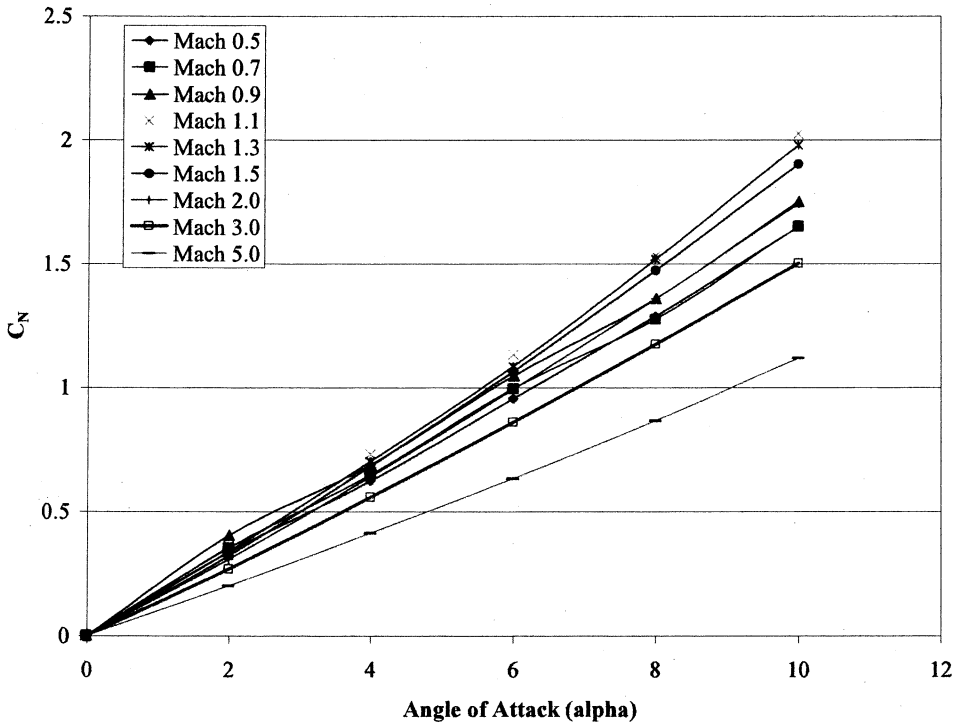

Figure 4.8 Normal Force Coefficients Calculated by Tiger CFD Code

CHAPTER V

FOUR VARIABLE RSM ANALYSIS OF A MISSILE

Completing a missile flight performance study is often very tedious, time consuming, and computationally intensive. While the engineer may know many characteristics about the missile, unknown properties can make the performance difficult to assess. A common method of replicating a missile flight is with a three degree of freedom computer model [2]. Aerodynamic coefficients are predicted by executing large sets CFD runs. The predicted aerodynamic coefficients as well as estimated missile properties are incorporated into the computer model as input parameters. The input parameters are varied and numerous Monte Carlo simulations are run to determine the envelope of missile trajectory, downrange distance, and time of flight. This process continues until the missile flight performance meets the qualifications designated by the analyst. Many times, thousands of simulation studies are run before the predetermined qualifications are met. The entire process is very computationally intensive and time consuming.

Response Surface Methods were applied to the generic three degree of freedom model, described in Chapter IV, to replicate the flight of a German V2 ballistic missile. Application of RSM with this model can reduce time to characterize the missile

performance envelope, predict future responses, and identify the parameters that influence the missile performance most. Three separate RSM studies were performed to evaluate this approach. The first analysis focused on four independent input variables. Two of the four variables in the first analysis interact within the missile model described in Chapter IV. The interactions and their influence on the simulation are discussed in this chapter. Within the second analysis, one of the two interacting variables was held constant while the remaining three variables were varied. The third analysis also examined three input variables. Two input variables from the first and second analyses remained while the variable that exhibited the least influence on the simulation was held constant and another variable was chosen in its place. Each of the three analyses contained the same two consistent variables throughout the study to serve as a parameter for comparison. The missile downrange distance in meters was the response factor for each of the analyses. The results from the three variable analyses are presented in Chapters VI and VII.

5.1 Calculation of Response Equation

To begin the first study, four independent variables were chosen to represent changes within the system. The variables specific impulse (ISP), mass flow rate ($\dot{m}$), pitchover gain and axial force coefficient scale factor (C_A) were assumed to impact the entire study the most. The specific impulse and mass flow rate interact within the propulsion module of the computer missile model. Due to this fact, an early assumption was made that the interactions between these two variables will have a greater influence on the simulation than any of the remaining variable interactions.

Because this study utilizes the 2^k CCD RSM techniques, a design matrix was established with high, nominal, and low values. Each of the assigned values, given in Table 5.1, were chosen from various resources about the V2 missile [15,16,17]. The specific impulse and mass flow rate values were determined using resource information concerning the missile engine and propellant type, while the pitchover gain values were determined from prior modeling and simulation experience. The predicted value for zero lift axial force coefficient (C_{AO}) is often estimated too high; therefore, the axial force coefficient scale factor (C_A) was always determined to be less than 1. This case only applies to aerodynamic data generated by computational means.

Table 5.1 Four Variable Analysis Levels

	ISP (sec)	**Mass Flow Rate (kg/s)**	**C_A**	**Pitchover Gain**
HIGH	211	140	0.85	0.7
LOW	209	120	0.75	0.5
NOMINAL	210	130	0.8	0.6

Table 5.2 Coded Matrix for Four Variable Analysis

Run	Level	ISP (sec) (x1)	Mass Flow Rate (kg/s) (x2)	C_A (x3)	Pitchover Gain (x4)
1	-1	-1	-1	-1	-1
2	a	1	-1	-1	-1
3	b	-1	1	-1	-1
4	ab	1	1	-1	-1
5	c	-1	-1	1	-1
6	ac	1	-1	1	-1
7	bc	-1	1	1	-1
8	abc	1	1	1	-1
9	d	-1	-1	-1	1
10	ad	1	-1	-1	1
11	bd	-1	1	-1	1
12	abd	1	1	-1	1
13	cd	-1	-1	1	1
14	acd	1	-1	1	1
15	bcd	-1	1	1	1
16	abcd	1	1	1	1
17		-2	0	0	0
18		2	0	0	0
19		0	-2	0	0
20		0	2	0	0
21		0	0	-2	0
22		0	0	2	0
23		0	0	0	-2
24		0	0	0	2
25		0	0	0	0

Once the input variables were chosen, the assigned values were placed into the model and the matrixes of simulations were run according to Table 5.2. Simulation runs 1 through 16 represent the corner points on the CCD cube of Figure 2.2 while runs 17 through 24 represent the axial points, and run 25 represents the center of the cube. The axial point location α, calculated using Equation (2.11), has a coded value of 2. The natural value for each variable, calculated with Equation (2.12), is given in Table 5.3. The level for each simulation run shown in Table 5.2 is used to determine the

influence of each variable on the overall simulation. This will be discussed further in the next section of this chapter.

Table 5.3 Four Variable α values

Coded Value	ISP (sec)	Mass Flow Rate(kg/s)	C_A	Pitchover Gain
-2	208	110	0.7	0.4
2	212	150	0.9	0.8

The simulations were executed in random order and the resulting downrange values were recorded. The results vector and coded matrix were then used to calculate the response equation characterizing the missile performance. The results vector and the simulation matrix using the natural variable values were used to create a natural response equation. The fitted response equation for the V2 missile system is given by

$$y = 252.08 + 4.05x_1 + 16.22x_2 - 3.07x_3 + 0.11x_4 + 0.005x_1x_2 - 0.035x_1x_3 + 0.003x_1x_4 - 0.01x_2x_3 - 0.01x_3x_4 + 0.79x_1^2 - 2.27x_2^2 - 1.27x_3^2 + 0.22x_4^2, \quad (5.1)$$

and the natural response equation is given by

$$y = 3341748 - 32848x_1 + 7.43x_2 + 859.40x_3 - 28.77x_4 + 0.0005x_1x_2 - 0.50x_1x_3 + 0.025x_1x_4 - 0.02x_2x_3 - 2.0x_3x_4 + 0.79x_1^2 - 0.023x_2^2 - 507.50x_3^2 + 21.88x_4^2. \quad (5.2)$$

Predicted downrange responses are calculated using Equation (5.1). The percent difference, or residual, was also calculated by comparing the predicted downrange results to the actual simulation results. A small residual signifies a small error, and thus a good response equation. A large residual signifies a large error and a relatively inaccurate

equation. The overall accuracy of the equation depends upon the application. For the missile performance assessment of this thesis, any residual below 10% is acceptable.

The residuals for this analysis range from 0% at the center of the cubic region to 4.99% located at the axial point of C_A. The low percentage of errors of the resulting residuals show that the downrange response equation is a reasonable representation of the simulated missile performance. This response equation may be used in the place of the numerous simulations typically performed. Each of the residual effects of the response equation is given in Table 5.4 and a graphical representation for the residuals is shown in Figure 5.1. All of the calculations for the four variable analysis are included in Appendix A.

Table 5.4 Comparison of Four Variable Simulation Results and RSM Equation

Simulation Run	Simulated Downrange	Predicted Downrange	Residual	Percent Difference
1	235.70	232.20	3.50	1.51%
2	244.56	240.34	4.22	1.75%
3	267.17	264.64	2.53	0.95%
4	276.12	272.80	3.32	1.22%
5	223.76	226.15	2.39	1.06%
6	232.58	234.19	1.61	0.69%
7	255.24	258.55	3.31	1.28%
8	264.03	266.61	2.58	0.97%
9	235.92	232.44	3.48	1.50%
10	244.80	240.59	4.21	1.75%
11	267.39	264.89	2.50	0.95%
12	276.34	273.06	3.28	1.20%
13	223.93	226.35	2.42	1.07%
14	232.77	234.40	1.63	0.70%
15	255.43	258.76	3.33	1.29%
16	264.22	266.83	2.61	0.98%
17	247.77	247.15	0.62	0.25%
18	260.96	263.36	2.40	0.91%
19	207.77	210.55	2.77	1.32%
20	276.48	275.41	1.07	0.39%
21	240.53	253.15	12.62	4.99%
22	251.71	240.87	10.84	4.50%
23	251.80	252.74	0.94	0.37%
24	252.34	253.19	0.85	0.34%
25	252.08	252.08	0.00	0.00%

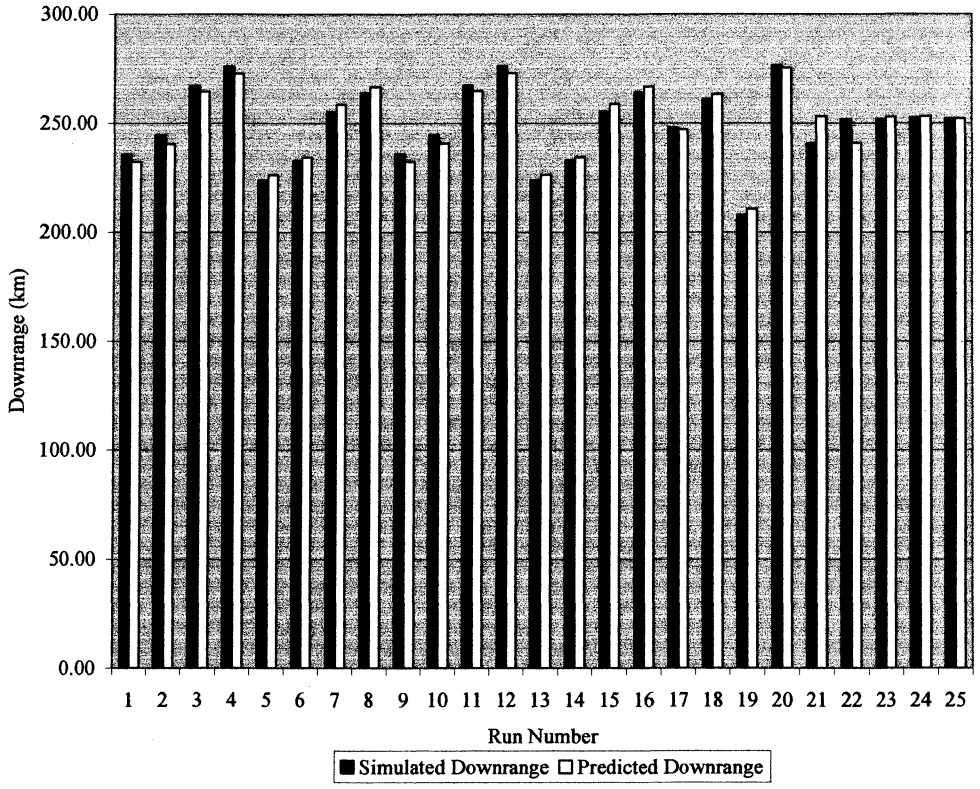

Figure 5.1 Four Variable Residual Errors

5.2 Variable Influence Determination

Characterizing the influence of each independent variable on the missile performance is a very important aspect of the RSM analysis. Equations (2.3) through (2.9) are used to determine the influence of each variable and the interactions between them. Another method of quickly determining the influence of each variable is by observing the magnitude of the associated coefficients within the response equation. The variable main values determined from Equations (2.3) through (2.9) along with each variable coefficient are each given in Table 5.5.

Table 5.5 Four Variable Main Influence Results

Variable	Variable Designator	Variable Main Influence	Variable Coefficient
ISP	A	21.018	4.050
MDOT	B	80.158	16.220
C_A	C	-21.193	-3.070
PITCH	D	0.545	0.110
ISP*MDOT	AB	0.020	0.005
ISP*C_A	AC	-0.100	-0.025
ISP*PITCH	AD	0.010	0.003
MDOT*C_A	BC	-0.040	-0.010
MDOT*PITCH	BD	0.000	0.000
C_A * PITCH	CD	-0.040	-0.010
ISP*ISP	AA	1.806	0.790
MDOT*MDOT	BB	8.477	-2.270
C_A*C_A	CC	0.021	-1.270
PITCH*PITCH	DD	0.123	0.220

Mass flow rate (MDOT) is the variable with the greatest influence on the overall simulation as indicated by the largest influence value and the largest coefficient. This means that the overall simulated missile performance is most affected when the value of MDOT is changed. By observing the role of the four variables within the simulation, it is clear why MDOT would have the most effect on the system. The mass flow rate is first used along with ISP, gravitational acceleration, nozzle exit area, and atmospheric pressure to calculate the thrust of the missile by Equation (4.1). MDOT is also used to determine the missile mass during flight. The mass and thrust of the missile are used throughout the simulation to determine the trajectory and final impact location of the missile.

The assumption that the ISP and MDOT interaction would have a significant influence on the missile performance was made at the beginning of the analysis. The low values of interaction coefficient and variable influence proved this assumption to be false. Although these two variables appear together in the missile performance, their interaction terms had very little influence on the overall simulation.

C_A and ISP have similar effects on the simulated missile performance. The pitchover gain variable has little effect on the overall performance when compared to the other input variables. To understand why this occurs, we go back to the original generic missile model. The pitchover gain is a means to increase or decrease the missile's pitch rate to reach an impact area. This variable has little influence on the actual maximum downrange achieved, but would possibly have a greater influence on the time it takes the missile to achieve a maximum downrange. In the third RSM analysis, this variable is replaced with the variable for launcher elevation angle.

What do these calculated influence results really tell an engineer? The variable with the greatest influence value will have a greater affect on the outcome of the simulation than will the other variables. Knowing which variable to vary or remove from the simulations can save time when determining missile system capabilities.

Response surface and contour plots were next created for the results of the four variable analyses. Responses relative to ISP and Mass Flow Rate, ISP and C_A, and C_A and Pitchover gain interactions are shown in the response surface and contour plots of Figures 5.2 through 5.7. The remainder of the plots is included in Appendix B.

No noticeable peak or valley is evident in the response surface plots of Figures 5.2, 5.4, and 5.6. This would lead one to believe that no maximum or minimum

response occurs at the stationary point of the overall system. Instead a saddle point is present at the stationary point location of the system. The contour plots of Figures 5.3, 5.5, and 5.7 verify this conclusion. If a maximum or minimum response were present at the stationary point of the system, the contour plots would contain a series of circles or ellipses radiating out from the center of the plot. Each of these plots shows an increase and decrease from the actual center point of the system, but no maximum or minimum occurs. This observation of the occurrence of a saddle point was next tested using ridge analysis.

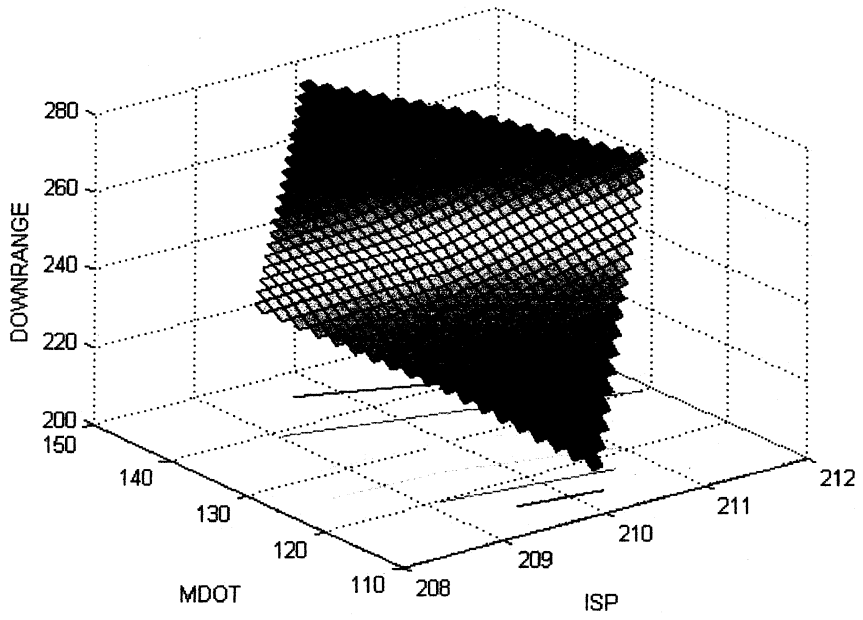

Figure 5.2 Four Variable Response Surface with Respect to ISP and Mass Flow Rate

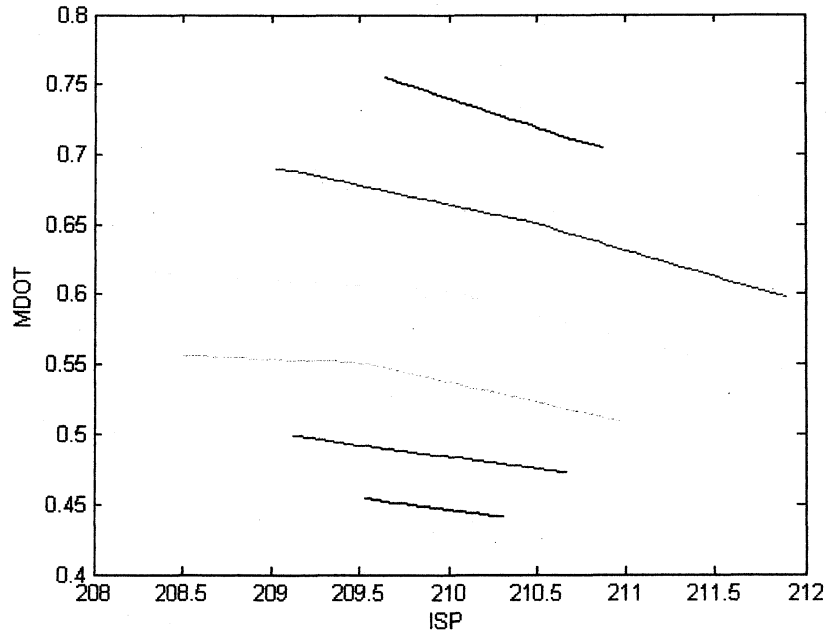

Figure 5.3 Four Variable Response Contour with Respect to ISP and Mass Flow Rate

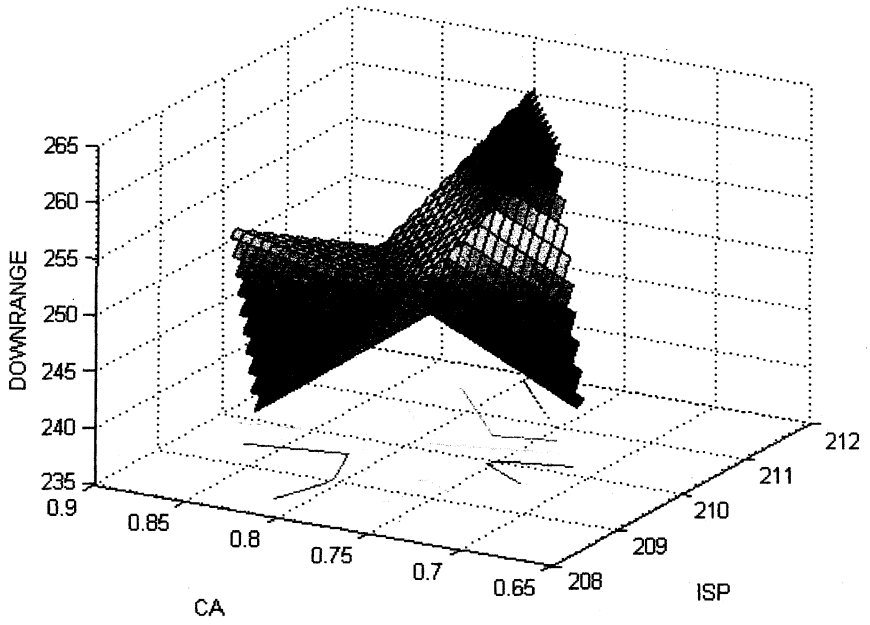

Figure 5.4 Four Variable Response Surface with Respect to ISP and C_A

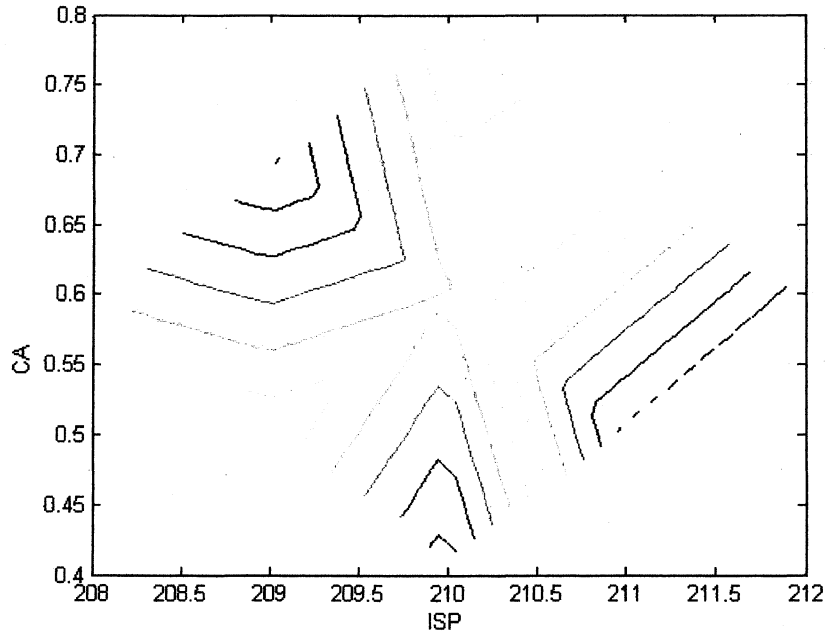

Figure 5.5 Four Variable Response Contour with Respect to ISP and C_A

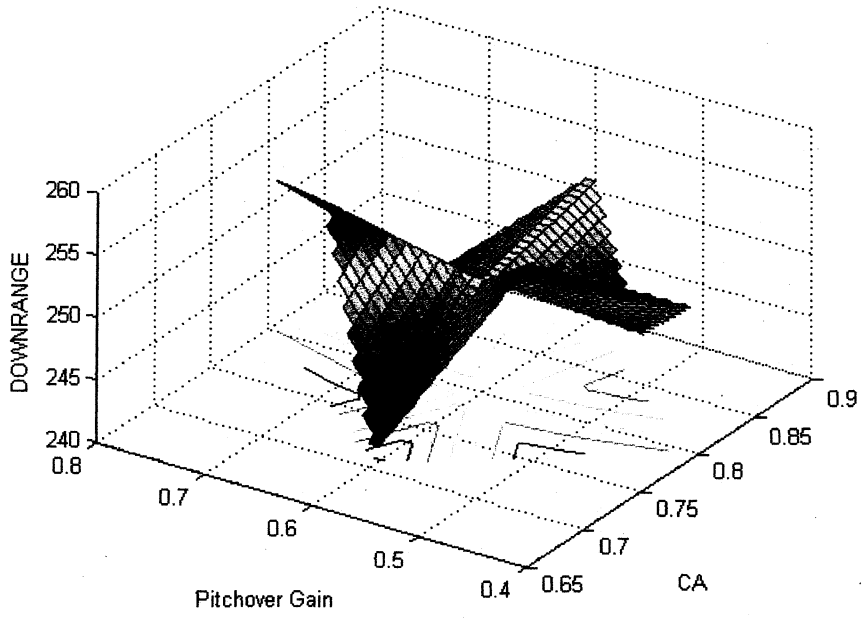

Figure 5.6 Four Variable Response Surface with Respect to Pitchover and C_A

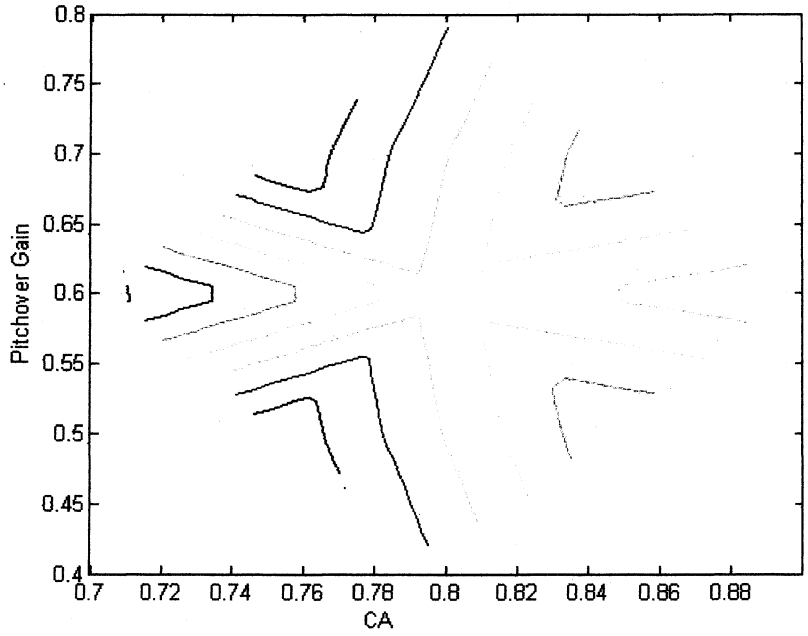

Figure 5.7 Four Variable Response Contour with Respect to Pitchover and C_A

5.3 Stationary Point and Ridge Analysis

The location and eigenvalues for the stationary point were calculated with Equations (2.13) through (2.15). The location of the stationary point of the simulation, shown in Table 5.6, lies outside of the area of variable exploration. The area of variable exploration is defined by the axial point locations of the RSM simulation matrix. The area of exploration for this study is defined between the axial point locations of -2 and 2. Because the eigenvalues have positive and negatives signs, neither a maximum nor minimum response occurs at the stationary point. This means that a saddle point is present at the center of the system. This proves that the observation from the response surface and contour plots was correct.

Table 5.6 Four Variable Analysis Stationary Point and Eigenvalue Results

Variable	Stationary Point	Eigenvalues
ISP	2.581	-2.2758
Mass Flow Rate	-3.5625	-1.2672
C_A	1.199	0.2204
Pitchover Gain	0.2696	0.7943

Since the stationary point of the entire simulation system was outside of the experimental region, it is of little use to the engineer. Ridge analysis must be performed to evaluate the response and investigate the behavior of the system within the specified region.

A ridge analysis study for maximum and minimum responses was completed for the four variable analysis. Constraint radii ranging from 0 to 2.0 in increments of 0.1 were placed around the stationary point of the system to define a perimeter with which to determine the maximum and minimum responses along with their respective stationary points. A Matlab code (provided in Appendix A) was written to perform the iterative process of determining the stationary point along with the maximum and minimum resulting downrange values that occur within each particular constraint radius within the defined area. Equations (2.17) and (2.18) were used as a basis for this analysis. Figure 5.8 and Table 5.7 demonstrate the observed maximum response behavior along each radius of constraint.

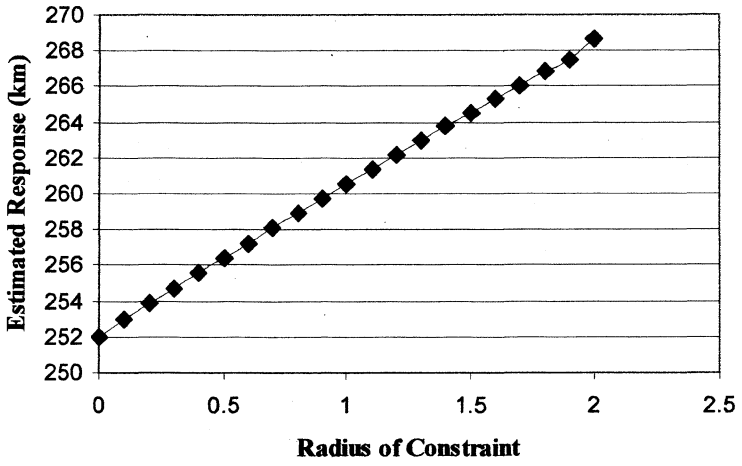

Figure 5.8 Radius Maximum Response Relations

Table 5.7 Ridge Analysis for a Maximum Response

Radius	Estimated Response	ISP (sec) x1	MDOT (kg/s) x2	C_A x3	Pitchover Gain x4	Standard Error of Prediction
0.0	252.01	0.00	0.00	0.00	0.00	13.52
0.1	253.01	0.03	0.10	-0.02	0.00	13.48
0.2	253.85	0.05	0.20	-0.04	0.00	13.39
0.3	254.70	0.08	0.29	-0.06	0.00	13.23
0.4	255.55	0.11	0.38	-0.08	0.00	13.01
0.5	256.40	0.15	0.48	-0.10	0.00	12.74
0.6	257.23	0.18	0.57	-0.12	0.00	12.41
0.7	258.07	0.22	0.66	-0.14	0.01	12.04
0.8	258.93	0.26	0.75	-0.16	0.01	11.61
0.9	259.73	0.31	0.83	-0.18	0.01	11.18
1.0	260.55	0.35	0.92	-0.20	0.01	10.71
1.1	261.38	0.41	1.00	-0.22	0.01	10.23
1.2	262.18	0.46	1.08	-0.24	0.01	9.77
1.3	262.96	0.52	1.16	-0.26	0.01	9.35
1.4	263.78	0.59	1.24	-0.28	0.01	8.98
1.5	264.52	0.65	1.31	-0.30	0.02	8.73
1.6	265.36	0.74	1.39	-0.32	0.02	8.62
1.7	266.04	0.81	1.45	-0.34	0.02	8.71
1.8	266.81	0.90	1.52	-0.36	0.02	9.04
1.9	267.50	0.99	1.58	-0.38	0.02	9.58
2.0	268.69	1.16	1.68	-0.41	0.03	11.13

As the constraint radius around the center of the stationary point location increases, the value of the resulting maximum response increases as well. At the origin of the radius, the downrange response value is approximately 252.08 km. This response is expected since the analysis begins with the fitted response equation having a linear intercept of 252.08 km.

Investigating Table 5.7 shows that the standard error of prediction calculated for the maximum responses along the radius of constraint ranged from a value of 8.62 at a radius location of 1.6 to a value of 13.52 at the center of the system. The errors decrease from the center of the system to a radius of 1.7 and then begin to increase until the constraint radius of 2.0 is reached. This change in error shows that the axial point locations chosen were not the best to represent the overall system. Although the axial point location for this study is 2, a better choice may be between 2.1 and 2.5. Using Equation (2.12), the change in axial point locations yields variable values of 212.1 to 212.5 for specific impulse, 151 to 155 for mass flow rate, 0.9 to 0.925 for axial force scale factor, and 0.755 to 0.775 for pitchover gain. To verify this assumption, the RSM analysis would need to be rerun with the new axial point locations and expansion of the constraint perimeter for ridge analysis.

Table 5.8 and Figure 5.9 illustrate the minimum response results occurring at the stationary point along each radius path. The minimum response along the path decreases as the radius from the origin becomes larger. The standard error of prediction was also calculated for each minimum estimated response. The pattern of the greatest error occurring at the center and the smallest error occurring at the 1.7 radius location is consistent with the maximum response results.

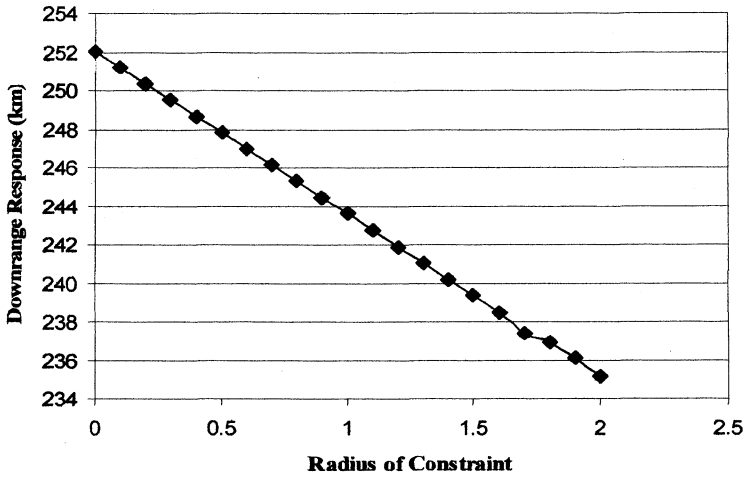

Figure 5.9 Radius Minimum Response Relations

Table 5.8 Ridge Analysis for a Minimum Response

Radius	Estimated Response	ISP (sec) x1	MDOT (kg/s) x2	C_A x3	Pitchover Gain x4	Standard Error of Prediction
0.00	252.01	0.00	0.00	0.00	0.00	13.90
0.10	251.21	-0.02	-0.10	0.02	0.00	13.87
0.20	250.37	-0.05	-0.19	0.04	0.00	13.77
0.30	249.52	-0.07	-0.29	0.05	0.00	13.61
0.40	248.67	-0.08	-0.39	0.07	0.00	13.39
0.50	247.82	-0.10	-0.48	0.09	0.00	13.11
0.60	246.98	-0.12	-0.58	0.10	0.00	12.78
0.70	246.14	-0.13	-0.68	0.12	0.00	12.40
0.80	245.30	-0.15	-0.77	0.13	0.00	11.98
0.90	244.43	-0.16	-0.87	0.15	0.00	11.51
1.00	243.62	-0.18	-0.97	0.16	-0.01	11.05
1.10	242.74	-0.19	-1.07	0.18	-0.01	10.53
1.20	241.88	-0.20	-1.17	0.19	-0.01	10.04
1.30	241.02	-0.21	-1.27	0.21	-0.01	9.59
1.40	240.19	-0.22	-1.37	0.22	-0.01	9.23
1.50	239.35	-0.24	-1.47	0.23	-0.01	8.97
1.60	238.50	-0.24	-1.57	0.25	-0.01	8.87
1.70	237.39	-0.26	-1.70	0.26	-0.01	9.04
1.80	236.92	-0.26	-1.75	0.27	-0.01	9.24
1.90	236.07	-0.27	-1.85	0.28	-0.01	9.78
2.00	235.12	-0.28	-1.97	0.30	-0.01	10.68

How does ridge analysis help the analyst determine the characteristics of this missile simulation? The ridge analysis secures the stationary point of the system within the experimental design region and applies a set of constraints for a particular set of variables. A constraint perimeter is placed around the stationary point. The maximum and minimum responses along with the variable locations corresponding to those responses are determined for different locations within the constraint perimeter. This helps the analyst choose the variable values needed to predict a specific downrange response. For example, using the four variable analysis, a maximum downrange is desired, but the missile must fly no less than 240 kilometers. Ridge analysis tells us that in order for the missile to achieve a maximum response but fly at least 240 kilometers, the engineer must look along the path of the 1.4 radius location from the origin. The maximum response along that path is approximately 263.78 kilometers. To achieve this response, values for each of the four study variables located within the simulation must be substituted with the variable values calculated during the ridge analysis study.

CHAPTER VI

THREE VARIABLE RSM ANALYSIS WITH PITCHOVER GAIN

Three variables were chosen for the second RSM study. Two variables, MDOT and ISP, in the four variable analysis are known to interact within a subsystem of the missile. To break this relation, ISP was held constant and the variable mass flow rate was retained. The remaining two variables for this analysis are C_A and Pitchover Gain.

6.1 Response Equation Calculations

The simulations were executed in the same manner as the four variable analysis, but the simulation matrix was based on a 2^3 factorial. With a decrease in number of variables from four to three, the size of the coded matrix and the number of runs needed to represent the system decreased. Using the CCD method eight initial runs were needed to represent the system, with the CCD two runs were needed to represent each axial or face centered point and one run was needed to represent the cube center. Table 6.1 displays the coded matrix for the three variable analyses and Table 6.2 contains the values assigned to each variable level.

The face centered points for this analysis were calculated using Equations (2.11) and (2.12). For a study with three variables (k=3), α has coded values of -1.682 and 1.682. The coded and natural axial point values are listed in Table 6.3.

Table 6.1 Coded Matrix for Three Variable Analysis With Pitchover Gain

Simulation Run	Level	Mass Flow Rate (kg/s) (x_1)	C_A (x_2)	Pitchover Gain (x_3)
1	1	-1	-1	-1
2	a	1	0	-1
3	b	-1	1	-1
4	ab	1	1	-1
5	c	-1	-1	1
6	ac	1	-1	1
7	bc	-1	1	1
8	abc	1	1	1
9		-1.682	0	0
10		1.682	0	0
11		0	-1.682	0
12		0	1.682	0
13		0	0	-1.682
14		0	0	1.682
15		0	0	0

Table 6.2 Levels for Three Variable Analysis With Pitchover Gain

	Mass Flow Rate (kg/s)	C_A	Pitchover Gain
HIGH	140	0.85	0.85
LOW	120	0.75	0.75
NOMINAL	130	0.7	0.8

Table 6.3 Three Variable Analysis With Pitchover Gain α Values

Coded Value	Mass Flow Rate (kg/s)	C_A	Pitchover Gain
-1.682	113.18	0.72	0.43
1.682	146.82	0.88	0.77

The simulations were executed in random order and the resulting downrange values were recorded. Equation (2.10) and the downrange results were then used to determine the response equations. The resulting coded response equation is

$$y = 252.05 + 16.04x_1 - 5.94x_2 + 0.11x_3 - 0.013x_1x_2 - 0.01x_2x_3 - 2.289x_1^2 + 0.09x_2^2 + 0.05x_3^2. \quad (6.1)$$

The resulting natural response equations is

$$y = -225.14 + 7.57x_1 - 176.53x_2 - 3.86x_3 - 0.026x_1x_2 - 2.00x_2x_3 - 0.02x_1^2 + 38.89x_2^2 + 5.49x_3^2. \quad (6.2)$$

The coded response equation was used to determine a predicted downrange for each of the given variables. Residual effects were then calculated by subtracting the predicted response values from the original simulation results. The simulation downrange result, predicted downrange result, and the residual error for each simulation run are listed in Table 6.4. The residuals are also graphically demonstrated in Figure 6.1. The largest residual occurs with simulation run 9 at the axial point location of mass flow rate variable while the smallest residual occurs with simulation run 15 at the center point of the cube. However, each of the residual errors of this analysis is significantly smaller than those from the four variable analysis. This is possibly caused by decreasing the number of variables used for the analysis. Even though the most influential variable was retained for this study, the greater the number of independent variables chosen for the analysis, the greater the risk of error in the response equation [2].

Table 6.4 Comparison of Simulation Results and RSM Equation for Three Variable Analysis With Pitchover Gain

Simulation Run	Simulated Downrange	Predicted Downrange	Residual	Percent Difference
1	240.11	239.67	0.44	0.18%
2	271.63	271.78	0.15	0.05%
3	228.16	227.84	0.32	0.14%
4	259.62	259.90	0.28	0.11%
5	240.34	239.92	0.42	0.17%
6	271.85	272.03	0.18	0.06%
7	228.34	228.05	0.29	0.13%
8	259.81	260.11	0.30	0.11%
9	217.8	218.60	0.80	0.37%
10	273.16	272.56	0.60	0.22%
11	262.06	262.31	0.25	0.09%
12	242.38	242.33	0.05	0.02%
13	251.88	252.01	0.13	0.05%
14	252.32	252.39	0.07	0.03%
15	252.05	252.05	0.00	0.00%

Small residual errors for the analysis show that the calculated response equation adequately represents the overall missile simulation. In future studies, this equation can be used to replace large numbers of simulation runs while trying to predict downrange results using other values for the independent variables.

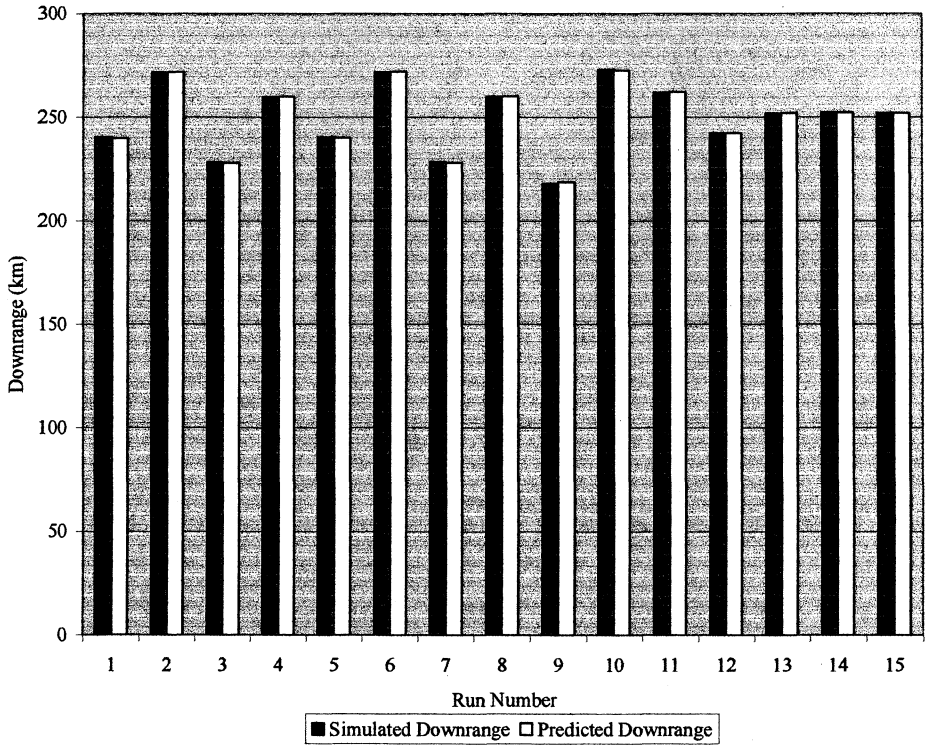

Figure 6.1 Three Variable Analysis With Pitchover Gain Residual Errors

6.2 Variable Influence Determination

The influence of each variable along with the variable interactions on the entire simulation was also investigated within the three variable analysis. Using Equations (2.3) through (2.9), the variable MDOT was determined to have the most influence on the overall simulation. This can also be seen by observing the variable coefficients of the response equation. Table 6.5 lists each of the calculated influence values for each variable along with the coefficients from Equation (6.1). As was the case of the four variable analysis, the MDOT variable has the most influence on the simulation and the PITCH variable has the least amount of influence on the overall simulation. This means that the overall simulation downrange result will be changed most when the value of

MDOT is varied and the simulation downrange result will be changed the least when the value of PITCH is changed.

Table 6.5 Three Variable Analysis With Pitchover Gain Main Influence Results

Variable	Variable Designator	Variable Main Influence	Variable Coefficient
MDOT	A	17.650	16.04
C_A	B	7.080	-5.94
PITCH	C	0.095	0.11
MDOT*C_A	AB	-0.025	-0.01
MDOT*PITCH	AC	0.000	0.00
C_A*PITCH	BC	-0.020	-0.01
MDOT*MDOT	AA	5.599	-2.29
C_A*C_A	BB	0.265	0.09
PITCH*PITCH	CC	0.158	0.05

The response surfaces and contours for each variable within the analysis were plotted to visually represent the behavior of the response surface represented by three independent variables. Figures 6.2 through 6.7 show the behavior of the simulation responses with respect to each variable combination. Similar to the four variable analysis, these plots appear to show that neither a maximum nor minimum response occurs at the stationary point. This observance will be proven when the calculated stationary point and eigenvalues are considered.

The response surface plots for MDOT and C_A and MDOT and Pitchover Gain (Figures 6.2 and 6.4) each appear to be linear. The contours of each (Figures 6.3 and 6.5) also show that the surface continues through the center of the system, but neither a maximum nor minimum occur. The response surface for C_A and Pitchover Gain (Figure 6.6) shows signs of curvature, but no significant peak or valley appears.

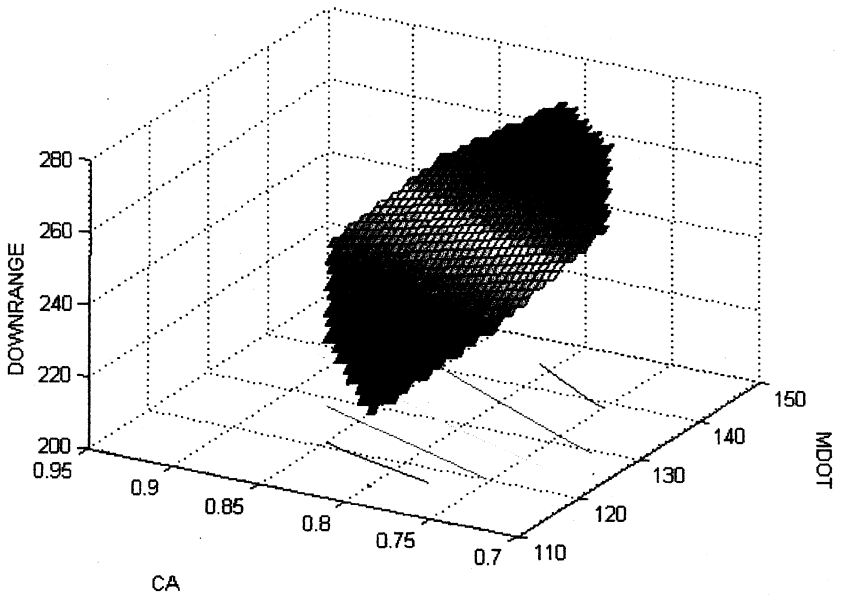

Figure 6.2 Three Variable Analysis With Pitchover Gain

Response Surface for MDOT vs. C_A

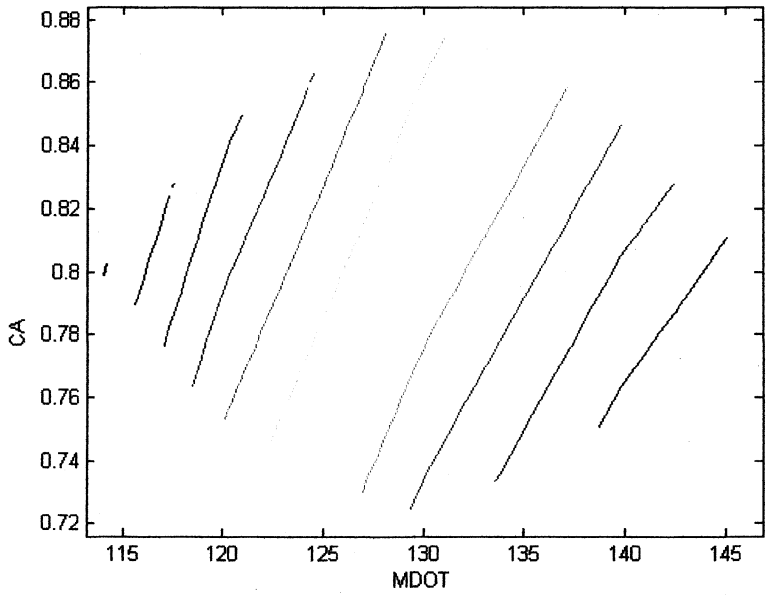

Figure 6.3 Three Variable Analysis With Pitchover Gain

Response Contour for MDOT vs. C_A

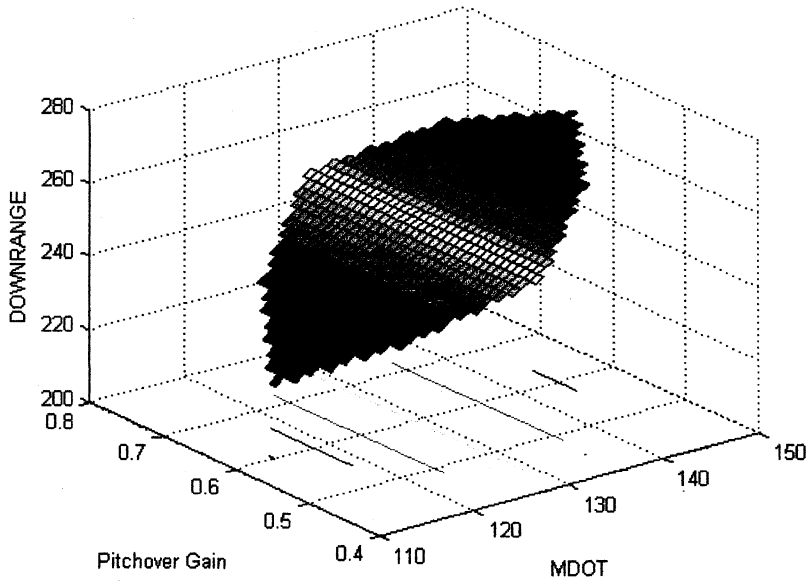

Figure 6.4 Three Variable Analysis With Pitchover Gain

Response Surface for MDOT vs. Pitchover Gain

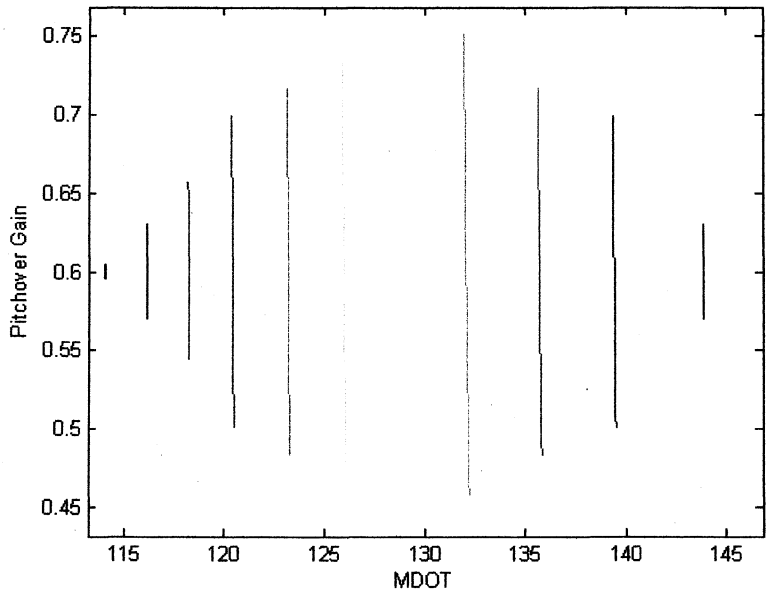

Figure 6.5 Three Variable Analysis With Pitchover Gain

Response Contour for MDOT vs. Pitchover Gain

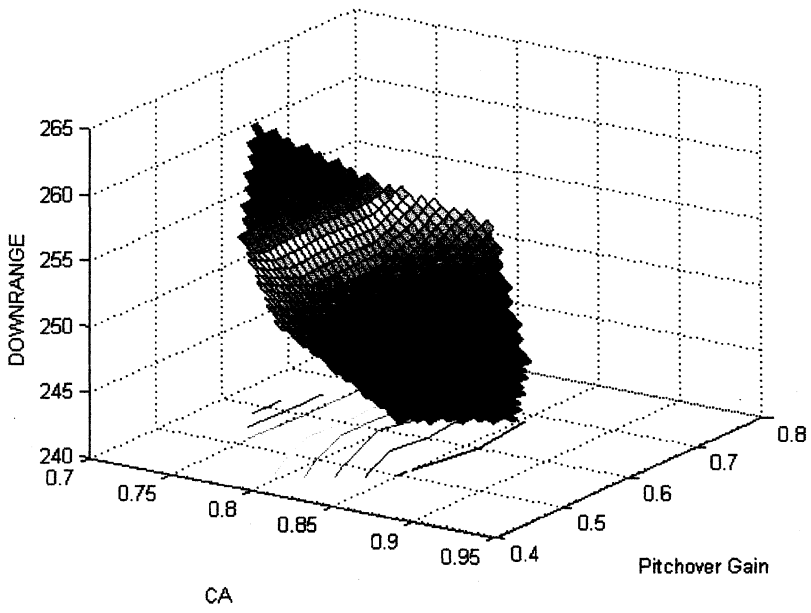

Figure 6.6 Three Variable Analysis With Pitchover Gain

Response Surface for C_A vs. Pitchover Gain

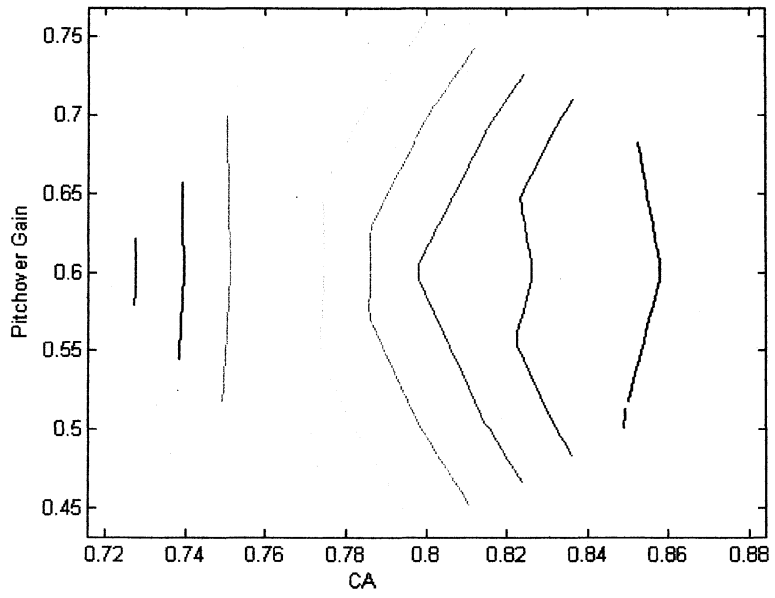

Figure 6.7 Three Variable Analysis With Pitchover Gain

Response Contour for C_A vs. Pitchover Gain

6.3 Stationary Point and Ridge Analysis

The location of the center point for the three variable analysis was determined in the same manner as that of the four variable analysis. The center of the response, or stationary point, can produce either a maximum response, minimum response, or neither. Equations (2.13) through (2.15) were used to determine the location of the stationary point and its significance to the analysis.

The location of the stationary point in reference to each of the three variables is given in Table 6.6. The calculated eigenvalues in reference to the stationary point are also included in Table 6.6. Two of the eigenvalues are negative and one is positive. This means that neither a maximum nor minimum response occurs at the stationary point of the system.

Table 6.6 Stationary Point and Eigenvalues for Three Variable Analysis with Pitchover Gain

Variable	Stationary Point	Eigenvalues
Mass Flow Rate	-3.409	-2.289
C_A	-33.3705	0.0494
Pitchover Gain	-2.237	0.0906

Since neither a maximum nor minimum response is achieved at the stationary point, ridge analysis was performed on the system. Radii from 0 to 2 units in increments of 0.1 units were theoretically placed around the stationary point of the system. The Matlab code for ridge analysis developed for the four variable analysis was modified for

this study and (Appendix C) was used to calculate each radius, estimate maximum and minimum responses, the position of that response relative to each of the three variables, and the standard error of the predicted value occurring at that location. Table 6.7 lists each of the maximum responses, their corresponding variable locations, and the standard error of prediction for each. As shown in the four variable analysis, when the size of the radius grows away from the center, the estimated maximum response grows. This increase of maximum response to the radius of constraint is demonstrated in Figure 6.8.

Table 6.7 Ridge Analysis Max. Response of Three Variable Analysis with Pitchover Gain

Radius	**Estimated Response**	**MDOT (kg/s) x1**	**C_A x2**	**Pitchover Gain x3**	**Standard Error of Prediction**
0.0	252.05	0.00	0.00	0.00	7.51
0.1	252.90	0.09	-0.04	0.00	7.48
0.2	253.76	0.19	-0.07	0.00	7.42
0.3	254.61	0.28	-0.11	0.00	7.30
0.4	255.47	0.37	-0.15	0.00	7.15
0.5	256.32	0.46	-0.20	0.00	6.95
0.6	257.17	0.55	-0.24	0.00	6.72
0.7	258.02	0.64	-0.29	0.01	6.47
0.8	258.86	0.72	-0.34	0.01	6.18
0.9	259.71	0.81	-0.39	0.01	5.89
1.0	260.55	0.89	-0.45	0.01	5.61
1.1	261.38	0.98	-0.51	0.01	5.36
1.2	262.21	1.06	-0.57	0.01	5.15
1.3	263.03	1.13	-0.63	0.01	5.02
1.4	263.85	1.21	-0.70	0.01	5.03
1.5	264.65	1.29	-0.77	0.02	5.18
1.6	265.45	1.36	-0.84	0.02	5.50
1.7	266.24	1.43	-0.92	0.02	5.99
1.8	267.02	1.50	-1.00	0.02	6.64
1.9	267.79	1.56	-1.08	0.02	7.42
2.0	268.54	1.63	-1.16	0.02	8.35

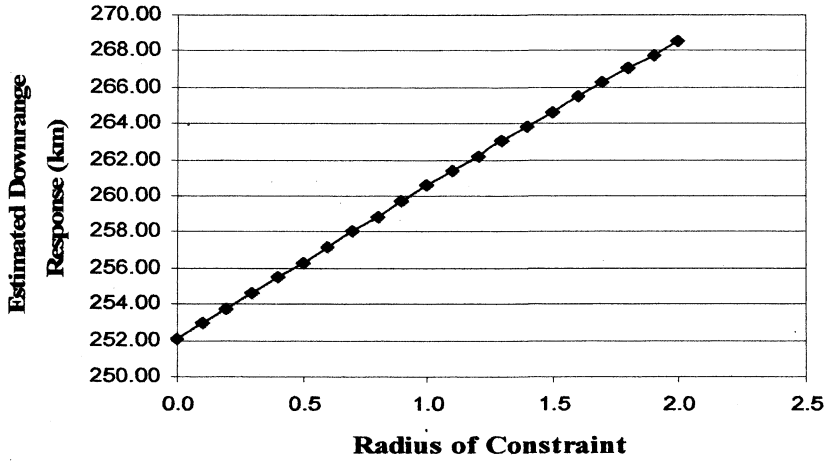

Figure 6.8 Radius of Constraint vs. Maximum Estimated Responses

The standard error at the center point is 7.51. This error decreases until the radius of 1.5 is reached and then begins to increase again until a radius of 2 units is achieved. The least error occurs at the 1.4 radius location with a maximum response of 263.85 kilometers. When a maximum response is wanted with a low risk of error, the recommended position would lie within the 1.4 radius range. Although this error is not identical to the four variable analysis, the trend remains unchanged.

The minimum response values determined for each radii were also calculated and are given in Table 6.8. The smallest minimum response of the system is located the farthest away from the center of the region. This trend is shown in Figure 6.9. The largest standard error of prediction also occurs at the perimeter of the region. If one were to seek a minimum response with a low risk of error, the region of interest would occur within the 1.4 radius region. This finding is consistent with that of the maximum response.

Table 6.8 Ridge Analysis Min. Response of Three Variable Analysis with Pitchover Gain

Radius	Estimated Response	MDOT (kg/s) x1	C_A x2	Pitchover Gain x3	Standard Error of Prediction
0.00	252.05	0.00	0.00	0.00	11.42
0.10	251.19	-0.09	0.03	0.00	11.39
0.20	250.34	-0.19	0.07	0.00	11.29
0.30	249.49	-0.28	0.10	0.00	11.11
0.40	248.63	-0.38	0.13	0.00	10.88
0.50	247.78	-0.48	0.15	0.00	10.58
0.60	246.93	-0.57	0.18	0.00	10.23
0.70	246.07	-0.67	0.21	0.00	9.84
0.80	245.22	-0.77	0.23	0.00	9.41
0.90	244.37	-0.86	0.25	0.00	8.97
1.00	243.52	-0.96	0.28	-0.01	8.54
1.10	242.68	-1.06	0.30	-0.01	8.15
1.20	241.83	-1.16	0.32	-0.01	7.83
1.30	240.99	-1.25	0.34	-0.01	7.65
1.40	240.14	-1.35	0.36	-0.01	7.65
1.50	239.29	-1.45	0.37	-0.01	7.88
1.60	238.45	-1.55	0.39	-0.01	8.37
1.70	237.61	-1.65	0.41	-0.01	9.11
1.80	236.77	-1.75	0.42	-0.01	10.09
1.90	235.93	-1.85	0.44	-0.01	11.29
2.00	235.10	-1.95	0.46	-0.01	12.68

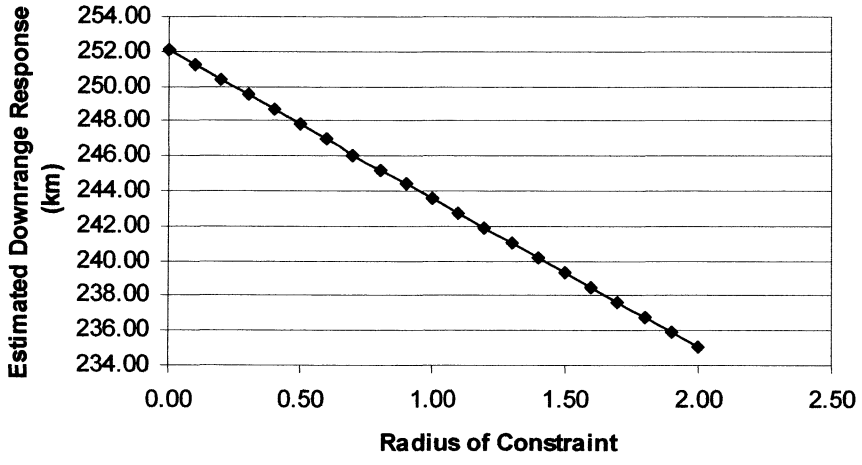

Figure 6.9 Radius of Constraint vs. Minimum Estimated Responses

This ridge analysis study can be used to predict future downrange responses by knowing the area to explore with the lowest risk of error. By determining the maximum and minimum responses along each radii within the predetermined constraint perimeter, behavior of the system response may be better understood.

CHAPTER VII

THREE VARIABLE RSM ANALYSIS WITH LAUNCHER ELEVATION ANGLE

Three variables were again chosen for the third RSM study. In the first two studies, the variable Pitchover Gain was shown to have very little significance to the overall missile simulations. For this reason, this variable was held constant during the third analysis and was replaced by a new variable, the Launcher Elevation Angle. The remaining two variables, MDOT and C_A, were retained for the third analysis.

7.1 Response Equation Calculations

Simulations were executed in the same manner as the two previous studies. Three independent variables are used in the third analysis; therefore, a 2^3 factorial design was applied. A total of 15 simulations is executed including the original 8 to represent the system and the center, and axial point locations for the CCD analysis. Table 7.1 presents the coded matrix for the three variable analyses and Table 7.2 contains the values assigned to each variable level.

The axial point locations for the three variable analysis with launcher elevation angle were calculated using Equations (2.11) and (2.12). Three independent variables were investigated within this analysis; therefore, k=3 and α = -1.682 and 1.682. These

axial point locations are represented with simulation runs 9-14 while the center point location is represented with simulation run 15.

Table 7.1 Coded Matrix for Three Variable Analysis with Launcher Elevation Angle

Simulation Run	**Level**	**Launcher Elevation Angle (degrees) (x_1)**	**Mass Flow Rate (kg/s) (x_2)**	**C_A (x_3)**
1	1	-1	-1	-1
2	a	1	0	-1
3	b	-1	1	-1
4	ab	1	1	-1
5	c	-1	-1	1
6	ac	1	-1	1
7	bc	-1	1	1
8	abc	1	1	1
9		-1.682	0	0
10		1.682	0	0
11		0	-1.682	0
12		0	1.682	0
13		0	0	-1.682
14		0	0	1.682
15		0	0	0

Table 7.2 Three Variable Analysis with Launcher Elevation Angle Levels

	Launcher Elevation Angle (degrees)	Mass Flow Rate (kg/s)	C_A
HIGH	80	140	0.85
LOW	60	120	0.75
NOMINAL	70	130	0.80

The simulations were executed in random order and the downrange values were recorded. The coded response equation derived is

$$y = 282.29 + 1.03x_1 + 15.81x_2 - 6.15x_3 + 0.26x_1x_2 + 0.009x_1x_3 - 0.071x_2x_3 - 0.18x_1^2 - 2.215x_2^2 + 0.06x_3^2, \quad (7.1)$$

and the natural response equation is

$$y = -174.2207 - 0.1953x_1 + 7.260x_2 - 146.3622x_3 + 0.0026x_1x_2 + 0.0175x_1x_3 - 0.01425x_2x_3 - 0.0018x_1^2 - 0.0221x_2^2 + 25.3895x_3^2. \quad (7.2)$$

The variable coefficients within the coded response equation provide an insight to which variables will influence the simulation most. The coefficient with the greatest magnitude represents the variable with the greatest influence on the overall simulation. By looking at Equation (7.1), the largest coefficient, 15.81, represents the mass flow rate variable (MDOT). This tells the engineer that the mass flow rate variable has the most influence on the simulation. The accuracy of this statement will be determined later within this chapter by calculating the main influence values from Equations (2.4) through (2.9).

Predicted downrange responses for each of the simulation runs were determined using the coded response equation. Residuals, given in Table 7.3 and graphically represented in Figure 7.1, were calculated by subtracting the predicted response values from the original simulation results. Residuals ranged from a minimum of 0.005 to a maximum of 0.803. The greatest residual occurs with simulation run 11 at the axial point location for mass flow rate and the smallest residual occurs with simulation run 14 at the axial point location for C_A. However, these residual error values are much smaller than

the residual errors from the four variable analysis and the three variable analysis with pitchover gain. Because of the small residual errors, the response equation from this analysis would be the preferred choice for predicted downrange values in relation to the three chosen independent variables.

Table 7.3 Simulation Results and Residual Effects for Three Variable Analysis with Launcher Elevation Angle

Simulation Run	Simulated Downrange	Predicted Downrange	Residual	Percent Difference
1	271.92	271.52	0.40	0.15%
2	269.37	268.94	0.43	0.16%
3	302.58	302.78	0.20	0.06%
4	301.08	301.23	0.15	0.05%
5	259.64	259.34	0.30	0.11%
6	257.14	256.79	0.35	0.14%
7	290.03	290.31	0.28	0.10%
8	288.55	288.80	0.25	0.09%
9	283.44	283.50	0.06	0.02%
10	279.89	280.05	0.16	0.06%
11	248.64	249.44	0.80	0.32%
12	303.23	302.64	0.59	0.20%
13	292.60	292.82	0.22	0.08%
14	272.13	272.12	0.01	0.002%
15	282.33	282.33	0.00	0.00%

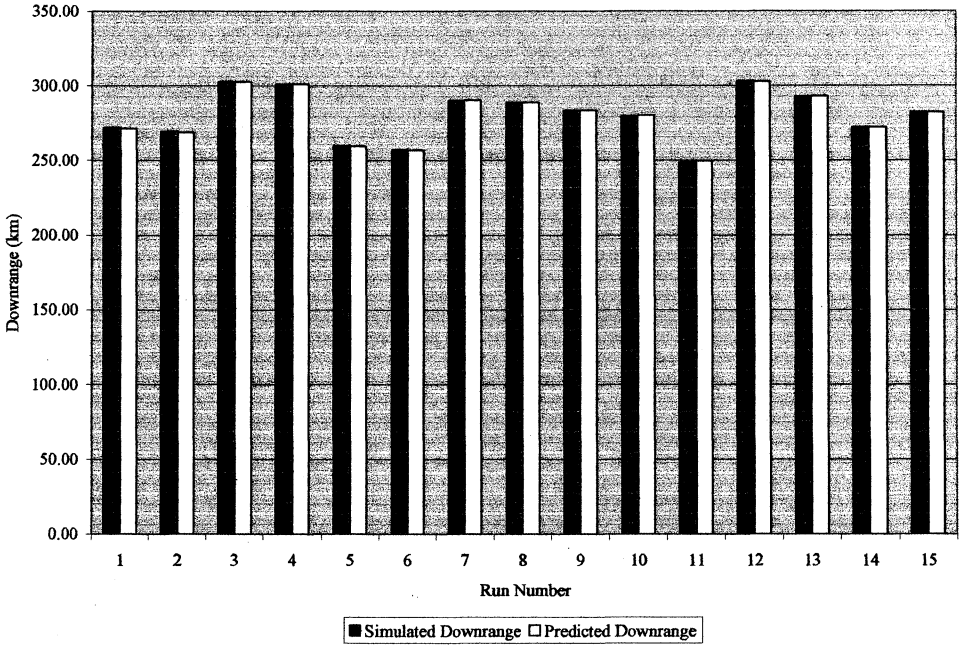

Figure 7.1 Three Variable Analysis With Launcher Elevation Angle Residual Errors

7.2 Variable Influence Determination

The effect of each variable on the entire simulation was calculated using Equations (2.3) through (2.9). Inspection of the coded response equation shows that the variable MDOT has the most influence on the missile performance. As with the first two analyses, the main influence results prove this to be true. Table 7.4 lists the main influence results along with the coefficients from the response equation for each variable and each variable interaction. The variable name listed in the table as LAUNCH represents the Launcher Elevation Angle.

Table 7.4 Main Influence Results for Three Variable Analysis

With Launcher Elevation Angle

Variable	Variable Designator	Variable Main Influence	Variable Coefficient
LAUNCH	A	2.68	1.03
MDOT	B	41.33	15.81
C_A	C	16.07	-6.15
MDOT*LAUNCH	AB	0.52	0.26
LAUNCH *C_A	AC	0.18	0.01
MDOT*C_A	BC	0.14	-0.07
LAUNCH*LAUNCH	AA	0.32	0.18
MDOT*MDOT	BB	3.84	-2.21
C_A*C_A	CC	0.11	0.06

The variable with the second greatest effect on the simulation is C_A. Because axial drag works along the body in a direction opposite to thrust, it is easy to see how this variable can effect the downrange of the missile more than the launcher elevation angle variable would.

The response surfaces and contours for each variable within the RSM analysis are represented in Figures 7.2 through 7.7. Response surface and contour plots are often used to quickly determine the behavior of a system, particularly near the stationary point of the system. As with the first two analyses, these plots appear to show that neither a maximum nor minimum response occurs at the stationary point. The response surface plots of Figures 7.2 and 7.6 show a linear surface with no noticeable peaks or valleys. Figure 7.4 exhibits a valley located near the center of the surface, but the contour plot of Figures 7.3, 7.5, and 7.7 indicates that no maximum or minimum response is shown in any of the plots. The assumptions made by visually observing the two- and

three-dimensional response surface plots can be verified using the stationary point and eigenvalue calculations.

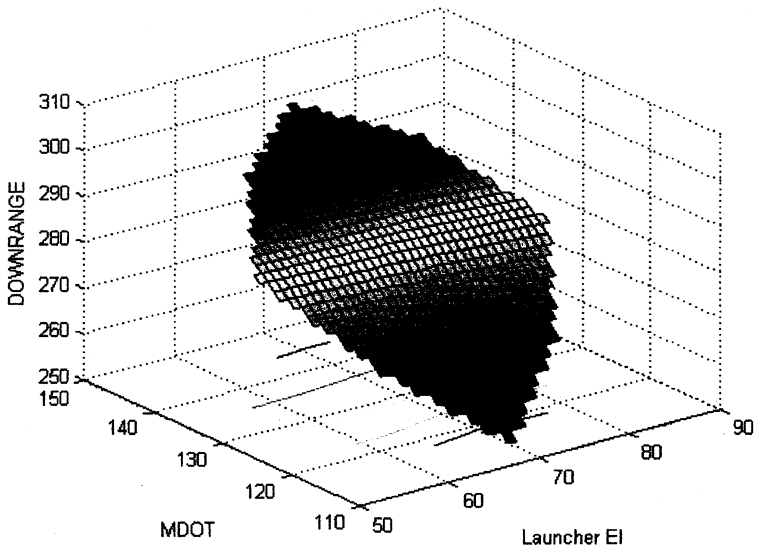

Figure 7.2 Three Variable Analysis With Launcher Elevation Angle

Response Surface for MDOT vs. Launcher Elevation Angle

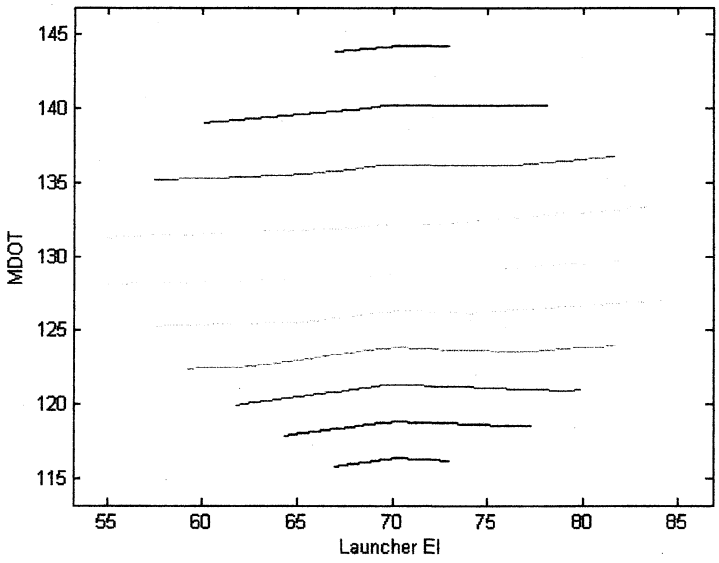

Figure 7.3 Three Variable Analysis With Launcher Elevation Angle

Response Contour for MDOT vs. Launcher Elevation Angle

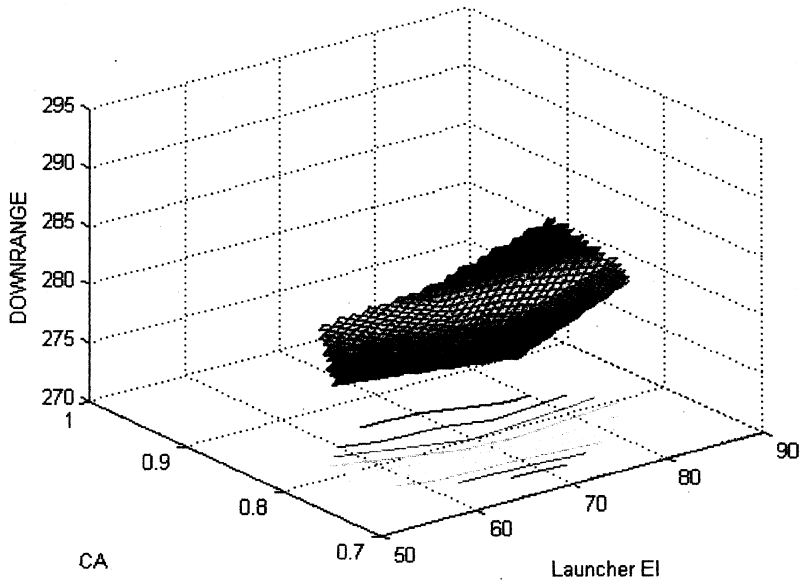

Figure 7.4 Three Variable Analysis With Launcher Elevation Angle

Response Surface for C_A vs. Launcher Elevation Angle

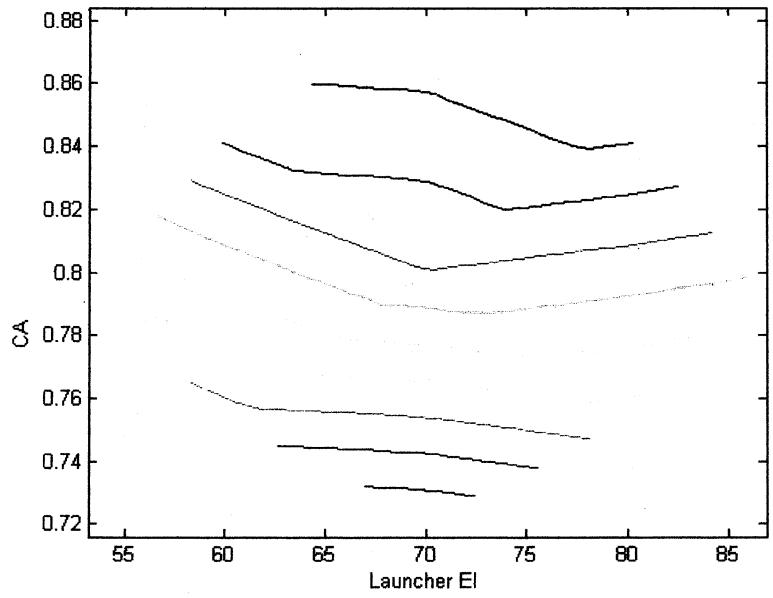

Figure 7.5 Three Variable Analysis With Launcher Elevation Angle

Response Contour for C_A vs. Launcher Elevation Angle

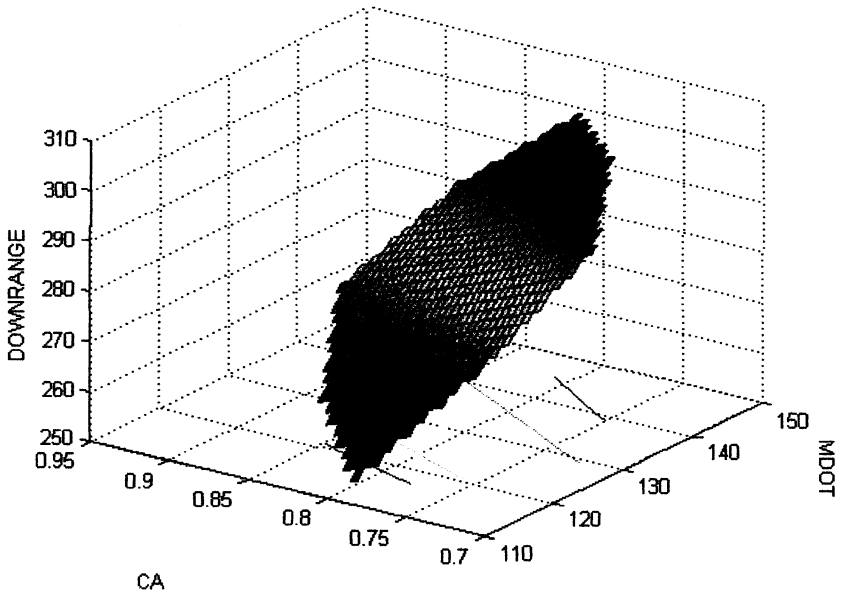

Figure 7.6 Three Variable Analysis With Launcher Elevation Angle

Response Surface for C_A vs. MDOT

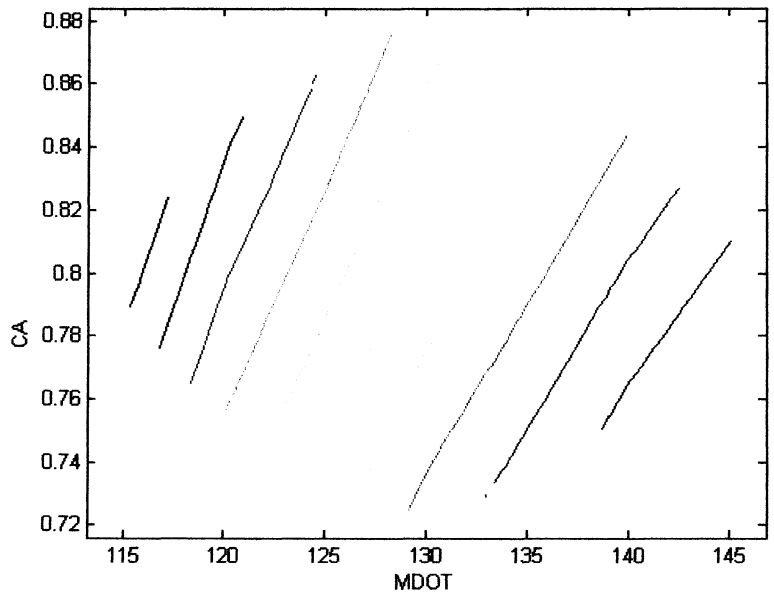

Figure 7.7 Three Variable Analysis With Launcher Elevation Angle

Response Contour for C_A vs. MDOT

7.3 Stationary Point and Ridge Analysis

The stationary point location for the second Three Variable Analysis was determined using Equations (2.13) through (2.15). Table 7.5 contains the stationary point location in respect to the three independent variables along with the resulting eigenvalues. Two of the calculated eigenvalues are negative and one, C_A, is positive. The eigenvalues having two different signs confirm the existence of neither a maximum nor minimum response at the stationary point of the system. The C_A variable yields a positive eigenvalue in each of the three studies. This shows that C_A is the variable that produces the saddle point for the analysis.

Table 7.5 Stationary Point and Eigenvalue Results for Three Variable Analysis With Launcher Elevation Angle

Variable	Stationary Point	Eigenvalues
Launcher Elevation Angle	-0.377	-2.2183
Mass Flow Rate	-2.7929	-0.176
CA Scale Factor	-50.1354	0.0639

Ridge analysis was applied to the system to determine its behavior around the stationary point location. A varying constraint radius was placed around the stationary point of the system with radii ranging from 0 to 2 units in increments of 0.1 units. The Matlab code written for the ridge analysis for the Three Variable Analysis with Launcher Elevation Angle (Appendix D) was used to iteratively determine the maximum and minimum responses for each radius value. The trend of the estimated maximum response for the radius of constraint is shown in Figures 7.8. Table 7.6 lists the estimated

maximum response, position of the response relative to each of the three variables, and the standard error of the predicted value for each radius location.

The results of this ridge analysis study are very similar to the previous two studies. As the size of the radius increases, the maximum response increases. The standard error located at the center of the system decreases until a radius of 1.4 is reached. Once the radius expands past this value, the error begins to increase again until a radius of 2 units is achieved, which is the edge of the perimeter. The smallest error for the maximum response study occurs at the 1.4 radius location with a maximum response of 294.02 kilometers and an error of 5.02. The maximum responses with the least error for each study are 265.36 with an error of 8.62 for the first study, 263.85 with an error of 5.03 for the second study, and 294.02 with an error of 5.02 for the third study.

The ridge analysis can lead the engineer toward an area of exploration for the variables within the analysis. Once the maximum and minimum responses along with the errors for each radii location are determined, the variable values essential to achieving a desired result are discovered.

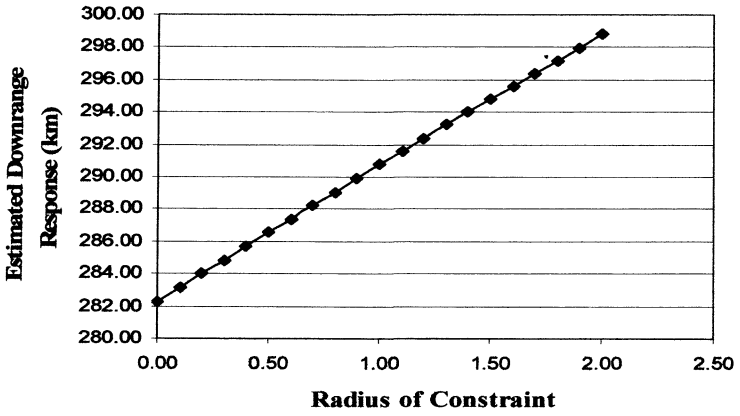

Figure 7.8 Three Variable Analysis with Launcher Elevation Angle Radius of Constraint vs. Maximum Estimated Responses

Table 7.6 Ridge Analysis for Maximum Response of Three Variable Analysis With Launcher Elevation Angle

Radius	Estimated Response	Launcher Elevation Angle (degrees) x1	Mass Flow Rate (kg/s) x2	C_A x3	Standard Error of Prediction
0.00	282.29	0.00	0.00	0.00	7.50
0.10	283.14	-0.01	0.09	-0.04	7.47
0.20	283.99	-0.01	0.18	-0.08	7.41
0.30	284.84	-0.02	0.28	-0.12	7.29
0.40	285.69	-0.02	0.37	-0.16	7.14
0.50	286.54	-0.03	0.46	-0.20	6.94
0.60	287.38	-0.04	0.54	-0.25	6.72
0.70	288.23	-0.04	0.63	-0.30	6.46
0.80	289.07	-0.05	0.72	-0.35	6.18
0.90	289.90	-0.05	0.80	-0.41	5.89
1.00	290.74	-0.06	0.88	-0.47	5.60
1.10	291.57	-0.06	0.97	-0.52	5.34
1.20	292.39	-0.07	1.04	-0.59	5.14
1.30	293.21	-0.07	1.12	-0.65	5.02
1.40	294.02	-0.08	1.20	-0.72	5.02
1.50	294.83	-0.08	1.27	-0.79	5.18
1.60	295.62	-0.09	1.34	-0.86	5.49
1.70	296.41	-0.09	1.41	-0.94	5.98
1.80	297.19	-0.10	1.48	-1.02	6.63
1.90	297.96	-0.10	1.55	-1.10	7.43
2.00	298.78	-0.11	1.62	-1.19	8.43

The minimum response values determined for each radius are given in Table 7.7 and the minimum response trend is shown in Figure 7.9. The minimum response along each radius location behaves in much the same manner as the maximum responses. The smallest minimum response of the system is located the farthest away from the center of the region. The largest standard error of prediction also occurs at the perimeter of the region. If one were to seek a minimum response with a low risk of error, the region of

interest would occur within the 1.4 radius region. This finding is consistent with that of the maximum response.

Table 7.7 Ridge Analysis for Minimum Response of Three Variable Analysis With Launcher Elevation Angle

Radius	Estimated Response	Launcher Elevation Angle (degrees) x1	Mass Flow Rate (kg/s) x2	C_A x3	Standard Error of Prediction
0.00	282.29	0.00	0.00	0.00	11.19
0.10	281.43	0.01	-0.09	0.04	11.16
0.20	280.59	0.01	-0.19	0.07	11.06
0.30	279.74	0.02	-0.28	0.10	10.89
0.40	278.89	0.02	-0.38	0.13	10.66
0.50	278.04	0.03	-0.47	0.16	10.37
0.60	277.19	0.04	-0.57	0.19	10.03
0.70	276.35	0.04	-0.67	0.22	9.64
0.80	275.50	0.05	-0.76	0.24	9.22
0.90	274.66	0.06	-0.86	0.27	8.79
1.00	273.74	0.06	-0.97	0.29	8.33
1.10	272.97	0.07	-1.05	0.31	7.98
1.20	272.13	0.07	-1.15	0.33	7.67
1.30	271.29	0.08	-1.25	0.35	7.50
1.40	270.45	0.09	-1.35	0.37	7.50
1.50	269.62	0.09	-1.45	0.39	7.73
1.60	268.78	0.10	-1.54	0.41	8.20
1.70	267.93	0.11	-1.64	0.43	8.94
1.80	267.11	0.11	-1.74	0.44	9.90
1.90	266.27	0.12	-1.84	0.46	11.09
2.00	265.43	0.12	-1.94	0.47	12.47

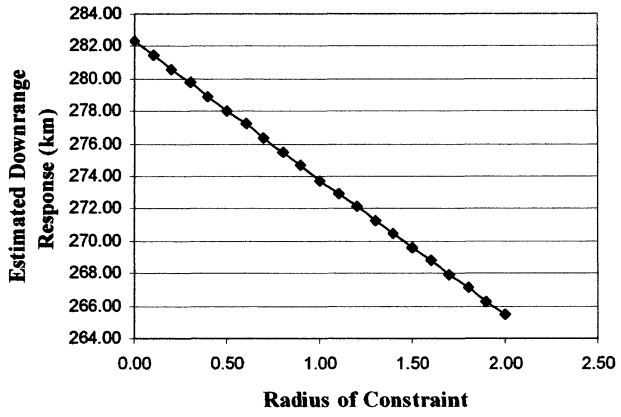

Figure 7.9 Three Variable Analysis With Launcher Elevation Angle Radius of Constraint vs. Minimum Estimated Responses

By observing the behavior of the standard error along each radius location, the conclusion is once again made that the axial distance of 1.682 used for the CCD analysis may not have been the appropriate value for this study. Since a distance of 2.0 was applied using the ridge analysis and the error value decreased until a point and then began to increase again, a value of 2.0 may have been better suited for the axial point locations within the CCD analysis. When an appropriate axial distance location is chosen for a system, the calculated standard error of prediction for that analysis will continue to decrease from the center of the system until it reaches the constrained perimeter. Given that the error of prediction is very dependant on the experimental design, the choice of the value 2.0 may have been better for the axial points of the analysis. Although a different choice for the axial point locations could provide a lower standard error of prediction as it nears the constraint perimeter, it will not affect the occurrence of the saddle point at the stationary point location.

CHAPTER VIII

SUMMARY AND CONCLUSION

This thesis addresses the applicability of the Response Surface Method (RSM) for characterizing missile performance. The analysis involved using RSM to predict downrange responses of a German V2 missile and identify influential parameters in a reasonable amount of time.

Three RSM studies were completed, each based on a different combination of input variables. The first study focused on four independent input variables, ISP, MDOT, C_A, and Pitchover Gain. Three variables were chosen for the second RSM study. Two variables, MDOT and ISP, in the four variable analysis are known to interact within the propulsion subsystem of the missile. To break this relation, ISP was held constant and the variable mass flow rate was retained. The remaining two variables for this analysis were C_A and Pitchover Gain. The third analysis also examined three input variables. In the first two studies, the variable Pitchover Gain was shown to have very little significance to the overall missile simulations. For this reason, this variable was held constant during the third analysis and was replaced by a new variable, the Launcher Elevation Angle. The remaining two variables, MDOT and C_A, were retained for the

third analysis. The missile downrange distance in meters was the response factor for each of the analyses.

The overall results from all three studies were very similar. The average residual errors for each study are 2.95, 0.286, and 0.281 consecutively. The large difference in residual highest residual error between the first analysis and the second and third analysis was primarily caused by the number of input variables of each. Four variables were used within the first analysis while three variables were used in the second and third analysis.

The lowest residual error occurs with the Three Variable Analysis with Launcher Elevation Angle analysis. The response equation calculated for this analysis most accurately represents the V2 missile simulation. This response equation, however, is valid only in the array of the assigned variables. As long as the same three variables are considered, the calculated response equation can be used to determine downrange results for other combinations not previously tested.

The mass flow rate was determined to have the most influence on the missile simulation in each analysis. By observing the role of each variable within the missile model, it is evident why mass flow rate has the greatest influence. The mass flow rate is used to determine thrust and current missile mass during the simulated flight. The thrust and missile mass are very important properties that are used throughout the simulation to determine velocity and location of the missile during flight.

Each study produced a saddle point at the stationary point location of the system. It is evident in each study that C_A was the driving factor for the occurrence of a saddle point. This was very predominant in the third study when the eigenvalue of C_A was the only positive eigenvalue. The eigenvalues of C_A were always positive in the three

analyses. The mass flow rate, ISP, and launcher elevation angle always produced negative eigenvalues.

The cause of the eigenvalues of C_A and mass flow rate having opposite signs can be explained in physical terms. The mass flow rate is used to determine mass and thrust during flight. Although the variable for mass flow rate is constant throughout flight, the resulting effects are not. Mass decreases during flight due to burning propellant while thrust decreases due to the propellant properties and mass.

C_{A0} theoretically opposes missile thrust during flight. The C_{A0} of the missile is dependent on the missile body shape; therefore, it does not change during flight. Because C_A is the scaling factor used to correct any over predicted C_{A0} data for the simulated missile flight and the C_A remains unchanged during the simulated flight, this would lead one to believe that the eigenvalues for C_A will always have a different sign than the eigenvalues of mass flow rate and will also cause a saddle point to occur in any RSM analysis of this missile model.

Although a saddle point does occur for each study, the ridge analysis calculations provide a method of predicting areas to pursue when trying to achieve desired maximum and minimum responses. Applying a constraint perimeter around the stationary point and calculating the maximum and minimum responses at various variable locations along with their error will show the analyst what the values of each variable must be in order to achieve a desired result.

Application of RSM techniques to missile simulations decreases the time needed to adequately explore the performance capabilities of a missile system. By using a single polynomial equation derived within the RSM process, thousands of simulation runs can

be neglected and variable influence may be investigated. Using ridge analysis for a system when a saddle point is present will guide the analyst toward the direction where each variable value must be set to achieve an anticipated result. Main influence calculations in RSM give the analyst the ability to focus on a set of variables that is known to have a major impact on the overall simulation response and neglect those variables that have very little impact on the response. Each of the capabilities provided through RSM will decrease the time needed to properly predict missile performance.

Future project efforts include the movement of axial point locations for each variable to determine their importance in establishing a standard error of prediction during ridge analysis. The overall scope of the project can also be increased to study other variables within each module of the missile performance model to anticipate the effect of the entire module on the overall simulation. A significant amount of time and resources would be needed to complete each of these tasks for the study of RSM analysis on missile simulations.

APPENDICES

APPENDIX A

FOUR VARIABLE ANALYSIS MATLAB CODES

```
Response Equations
%-------------------------------------------------------------------
%Study A
%This m-file was created to calculated the coded and natural response
% equations for the V2 simulation.
%-------------------------------------------------------------------
% Coded Matrix
% A:ISP
% B:MDOT
% C:CASCALE
% D:PITCHOVER
%-------------------------------------------------------------------
%-------------------------------------------------------------------
I=[1;1;1;1;1;1;1;1;1;1;1;1;1;1;1;1;1;1;1;1;1;1;1;1;1;1;1];
A=[-1;  1;  -1; 1;  -1; 1;  -1; 1;  -1; 1;  -1; 1;  -1; 1;  -1;1; ...
   -2; 2; 0;   0;  0;  0;  0;  0;  0;  0];
B=[-1;  -1; 1;  1;  -1; -1; 1;  1;  -1; -1; 1;  1;  -1; -1; 1; ...
   1;  0;  0;  -2; 2;  0;  0;  0;  0;  0];
C=[ -1; -1; -1; -1; 1;  1;  1;  1;  -1; -1; -1; -1; 1;1;...
   1;  1;  0;  0;  0;  0;  -2; 2;  0;  0;  0];
D=[-1;  -1; -1; -1; -1; -1; -1; -1; 1;  1;  1; 1; 1; 1;  1;...
   1;  0;  0;  0;  0;  0;  0;  -2; 2;  0];
AA=A.*A;
BB=B.*B;
CC=C.*C;
DD=D.*D;
AB=A.*B;
AC=A.*C;
AD=A.*D;
BC=B.*C;
BD=B.*D;
CD=C.*D;
ABC=A.*B.*C;
ABD=A.*B.*D;
ACD=A.*C.*D;
BCD=B.*C.*D;
ABCD=A.*B.*C.*D;
X1=[I A B C D AB AC AD BC BD CD AA BB CC DD];
y=[235.7;244.56;267.17;276.12;223.76;232.58;255.24;264.03;235.92;244.8;...
```

```
  267.39;276.34;223.93;232.77;255.43;264.22;247.77;260.96;207.77; ...
  276.4;240.53; 251.71;251.8;252.34;252.08];
b1=(inv(X1'*X1))*X1'*y;
Yprime1=X1*b1
error1=y-Yprime1;
%-------------------------------------------------------------------------
%Actual Matrix

% M:ISP
% N:MDOT
% O:CASCALE
% P:PITCHOVER
%-------------------------------------------------------------------------
L=[1;1;1;1;1;1;1;1;1;1;1;1;1;1;1;1;1;1;1;1;1;1;1;1;1;1;1;1;1;1;1;1];
M=[209;211;209;211;209;211;209;211;209;211;209;211;209;211;209;211;208; ...
     212;210;210;210;210;210;210;210];
N=[120;120;140;140;120;120;140;140;120;120;140;140;120;120;140;140;130;...
     130; 110;150;130;130;130;;130;130];
O=[0.75;0.75;0.75;0.75;0.85;0.85;0.85;0.85;0.75;0.75;0.75;0.75;0.85; ...
    0.85; 0.85;0.85;0.8;0.8;0.8;0.8;0.7;0.9;0.8;0.8;0.8];
P=[0.5;0.5;0.5;0.5;0.5;0.5;;0.5;0.5;0.7;0.7;0.7;0.7;0.7;0.7;0.7;0.7;0.6; ...
   0.6;0.6;0.6;0.6;0.6;0.4;;0.8;0.6];
MM=M.*M;
NN=N.*N;
OO=O.*O;
PP=P.*P;
MN=M.*N;
MO=M.*O;
MP=M.*P;
NO=N.*O;
NP=N.*P;
OP=O.*P;
MNO=M.*N.*O;
MNP=M.*N.*P;
MOP=M.*O.*P;
NOP=N.*O.*P;
MNOP=M.*N.*O.*P;
J1=[I M N O P MN MO MP NO NP OP MM NN OO PP];
J2=[I M N O P MN MO MP NO NP OP MM NN OO PP MNO MNP MOP NOP
MNOP];
c1=(inv(J1'*J1))*J1'*y;
Jprime1=J1*c1;
errorJ1=y-Jprime1

Main Effects Calculations
%-------------------------------------------------------------------------
```

```
% This m-file was created to calculate the main effects and Sum of Squares
% for each variable V2 simulation RSM
%------------------------------------------------------------------------
%------------------------------------------------------------------------
n=1;
l=235.7;
 a=244.56;
 b=267.17;
 ab=276.12
 c=223.76;
 ac=232.58;
 bc=255.24;
 abc=264.03;
 d=235.92;
 ad=244.8;
 bd=267.39;
 abd=276.34;
 cd=223.93;
 acd=232.77;
 bcd=255.43;
 abcd=264.22;

 aa=260.96;
 bb=276.48;
 cc=251.71;
 dd=252.34;
 naa=247.77;
 nbb=207.77;
 ncc=240.44;
 ndd=251.8;

G=1/(4*n);
m=16*n;
A=G*((a+ac+abc+ab+ad+abd+acd+abcd+aa)-(b+c+bc+d+bd+cd+bcd+l+naa));
B=G*((b+ab+bc+abc+bd+abd+bcd+abcd+bb)-(a+c+ac+d+ad+cd+acd+l+nbb));
C=G*((c+ac+bc+abc+cd+acd+bcd+abcd+cc)-(a+b+ab+d+ad+bd+abd+l+ncc));
D=G*((d+ad+bd+abd+cd+acd+bcd+abcd+dd)-(a+b+ab+c+ac+bc+abc+l+ndd));
AB=G*((l+ab+c+abc+d+abd+cd+abcd)-(b+a+ac+bc+ad+bd+acd+bcd));
AC=G*((l+b+ac+abc+d+bd+acd+abcd)-(a+ab+c+bc+ad+abd+cd+bcd));
AD=G*((l+b+c+bc+ad+abd+acd+abcd)-(a+ab+ac+abc+d+bd+cd+bcd));
BC=G*((l+a+bc+abc+d+ad+bcd+abcd)-(b+ab+c+ac+bd+abd+cd+acd));
BD=G*((l+a+c+ac+bd+abd+bcd+abcd)-(b+ab+bc+abc+d+ad+cd+acd));
CD=G*((l+a+b+ab+cd+acd+bcd+abcd)-(c+ac+bc+abc+d+ad+bd+abd));
ABD=G*((a+b+ac+bc+d+abd+cd+abcd)-(l+ab+c+abc+ad+bd+acd+bd));
ABC=G*((a+b+c+abc+ad+bd+cd+abcd)-(l+ab+ac+bc+d+cd+acd+bd));
ACD=G*((a+ab+c+bc+d+bd+acd+abcd)-(l+b+ac+abc+ad+abd+cd+bd));
```

```
BCD=G*((ab+c+ac+b+d+ad+bd+abcd)-(l+a+bc+abc+bd+abd+cd+acd));
ABCD=G*((l+ab+ac+bc+ad+bd+cd+abcd)-(a+b+c+abc+d+abd+acd+bd));
Q=[A;B;C;D;AB;AC;AD;BC;BD;CD;ABD;ABC;ACD;BCD;ABCD];


SSA=(((a+ac+abc+ab+ad+abd+acd+abcd+aa)-(b+c+bc+d+bd+cd+bcd+l+naa))^2)/m;
SSB=(((b+ab+bc+abc+bd+abd+bcd+abcd+bb)-(a+c+ac+d+ad+cd+acd+l+nbb))^2)/m;
SSC=(((c+ac+bc+abc+cd+acd+bcd+abcd+cc)-(a+b+ab+d+ad+bd+abd+l+ncc))^2)/m;
SSD=(((d+ad+bd+abd+cd+acd+bcd+abcd+dd)-(a+b+ab+c+ac+bc+abc+l+ndd))^2)/m;

SSAB=(((l+ab+c+abc+d+abd+cd+abcd)-(b+a+ac+bc+ad+bd+acd+bcd))^2)/m;
SSAC=(((l+b+ac+abc+d+bd+acd+abcd)-(a+ab+c+bc+ad+abd+cd+bcd))^2)/m;
SSAD=(((l+b+c+bc+ad+abd+acd+abcd)-(a+ab+ac+abc+d+bd+cd+bcd))^2)/m;
SSBC=(((l+a+bc+abc+d+ad+bcd+abcd)-(b+ab+c+ac+bd+abd+cd+acd))^2)/m;
SSBD=(((l+a+c+ac+bd+abd+bcd+abcd)-(b+ab+bc+abc+d+ad+cd+acd))^2)/m;
SSCD=(((l+a+b+ab+cd+acd+bcd+abcd)-(c+ac+bc+abc+d+ad+bd+abd))^2)/m;
R=[SSA;SSB;SSC;SSD;SSAB;SSAC;SSAD;SSBC;SSBD;SSCD]
```

```
Stationary Point and Ridge Analysis Calculations
%-------------------------------------------------------------------------
% This program is designed to calculate the stationary point of the
% response surface and determine if it is a maximum or minimum point.
%-------------------------------------------------------------------------
%y1 =252.0800+4.0525*A+16.2158*B-3.0700*C+0.1133*D+0.0050*AB-0.0250*AC+
%    0.0025*AD-0.0100*BC-0.0100*CD+0.7942AA-2.2758*BB-1.2671CC+0.2204DD
%-------------------------------------------------------------------------
% Study A coded matrix
%-------------------------------------------------------------------------
b11=0.7942;
b22=-2.2758;
b33=-1.2671;
b44=0.2204;
b12=0.005;
b13=-0.025;
b14=0.0025;
b23=-0.01;
b24=0;
b34=-0.01;
b=[4.0525;16.2158;-3.0700;0.1133];
Bhat=[b11 b12/2 b13/2 b14/2;b12/2 b22 b23/2 b24/2;b13/2 b23/2 b33 b34/2;b14/2 b24/2
b34/2 b44];
Xs_AC=0.5*(inv(Bhat))*b;
%Xs_AC=[7.8988;0.3733;-20.1364;0.2844];
if (eig(Bhat))>1
   'point is a minimum'
else if (eig(Bhat))<1
       'point is a maximum'
   else
      'point is neither'
   end
end
ys_A=252.08+0.5*(Xs_AC)'*b;
% %-------------------------------------------------------------------------
% % Study A Ridge Analysis Iteration
% %-------------------------------------------------------------------------
L=0.195;
U=0.2019;
lambda=-3.5
for l=0:0.05:1000
   lambda_x=lambda-l;
   x_bar=(inv(Bhat-lambda_x*eye(4)))*(-0.5*b)
   R=sqrt(x_bar'*x_bar);
   H=R>L;
   S=R<U;
```

```
   if and (H,S)
   break
   else
      continue
end
end
R
ysA=252.08+0.5*(x_bar)'*b

yhat=x_bar'*b
```

APPENDIX B

FOUR VARIABLE ANALYSIS PLOTS

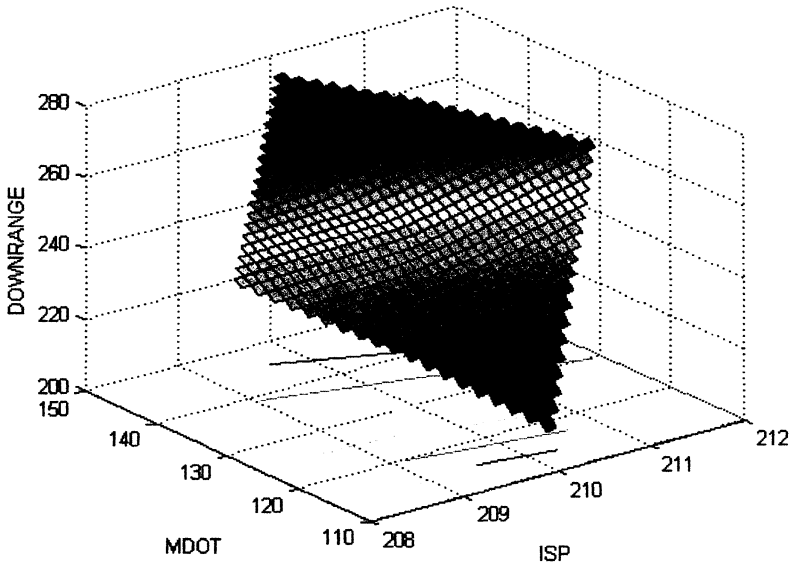

Figure B.1 Response Surface MDOT vs. ISP

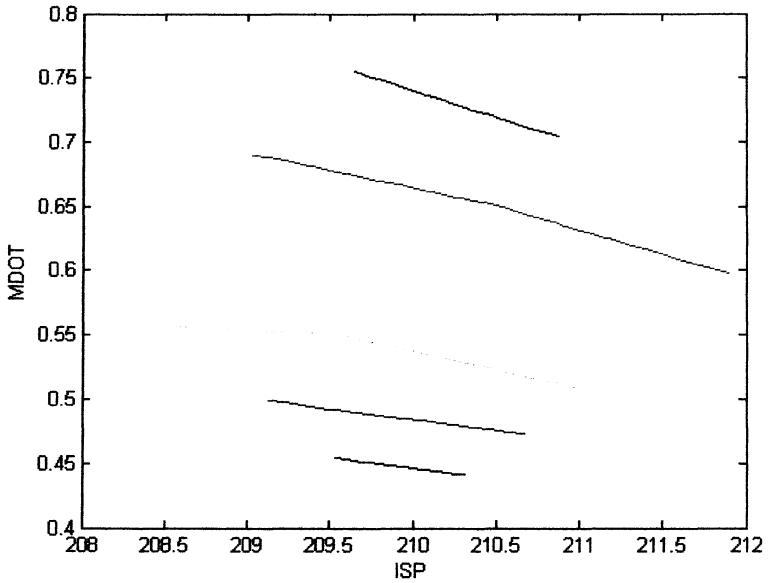

Figure B.2 Contour Plot MDOT vs. ISP

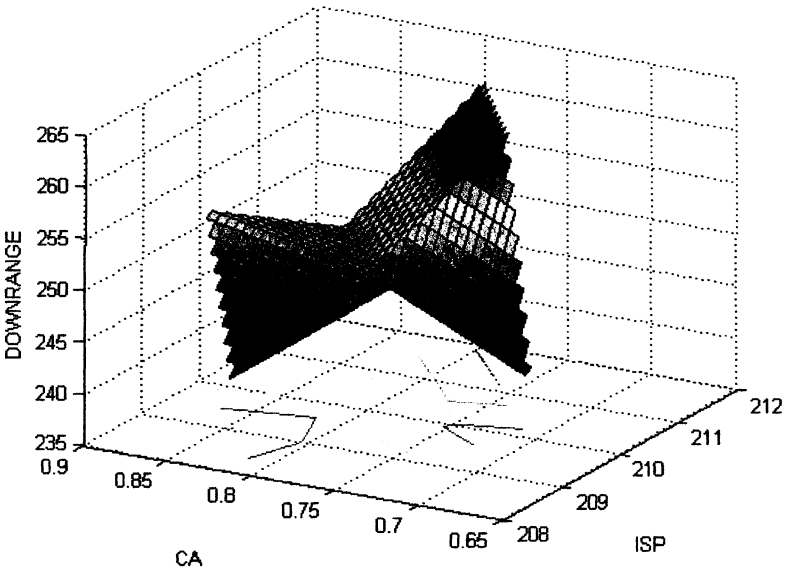

Figure B.3 Response Surface Plot C_A vs. ISP

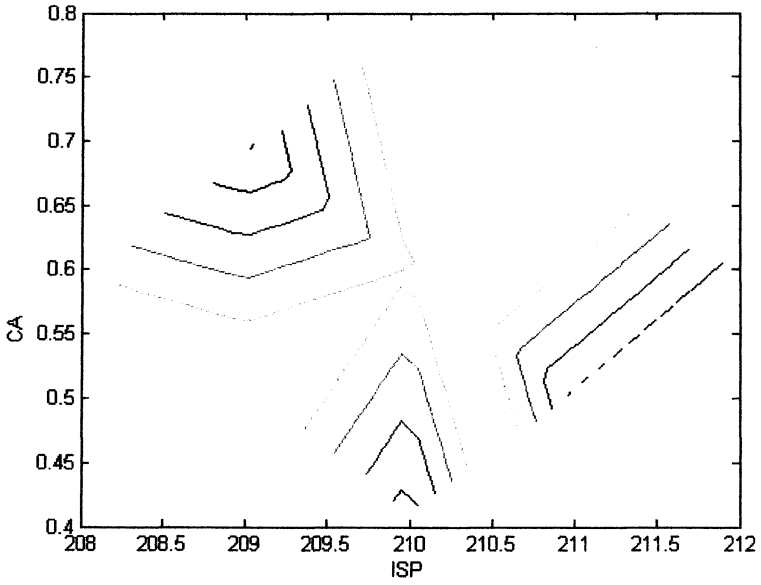

Figure B.4 Contour Plot C_A vs. ISP

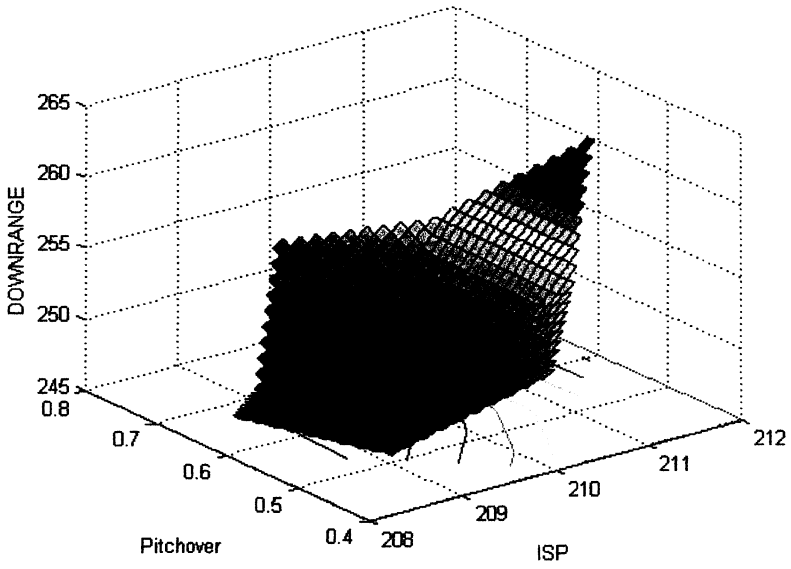

Figure B.5 Response Surface Plot Pitchover vs. ISP

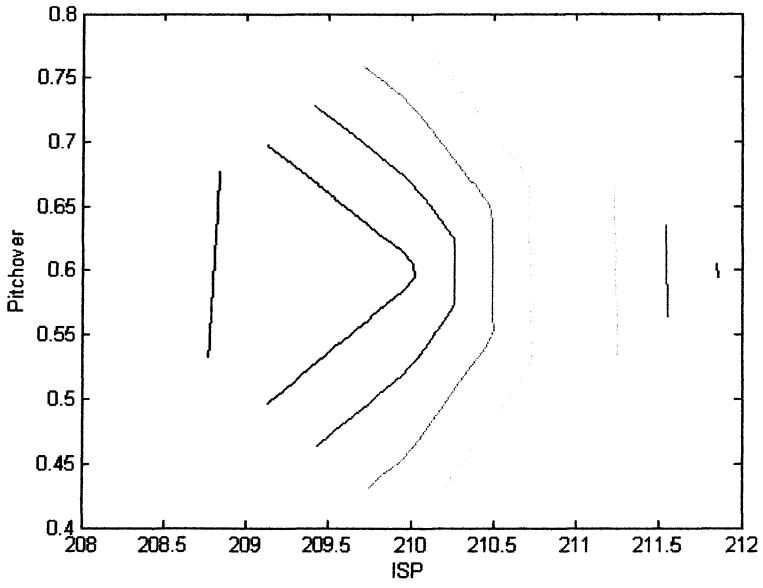

Figure B.6 Contour Plot Pitchover vs. ISP

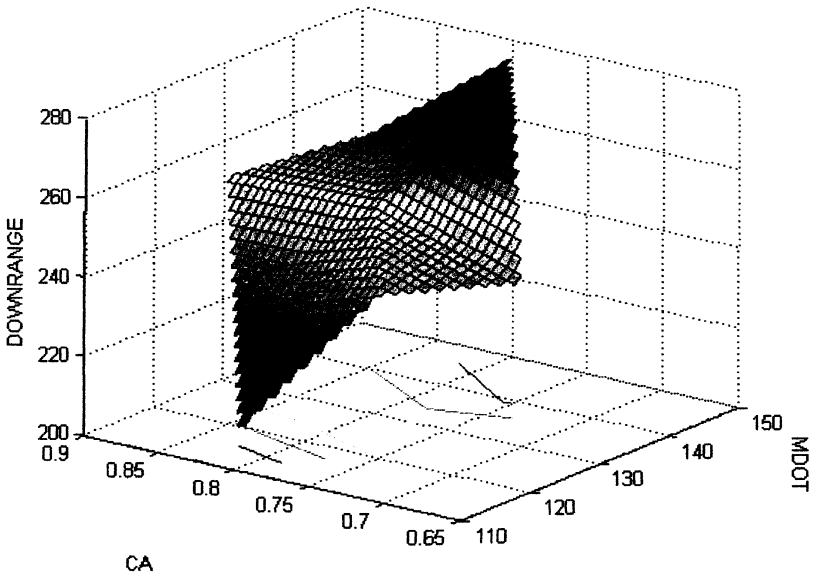

Figure B.7 Response Surface Plot C_A vs. MDOT

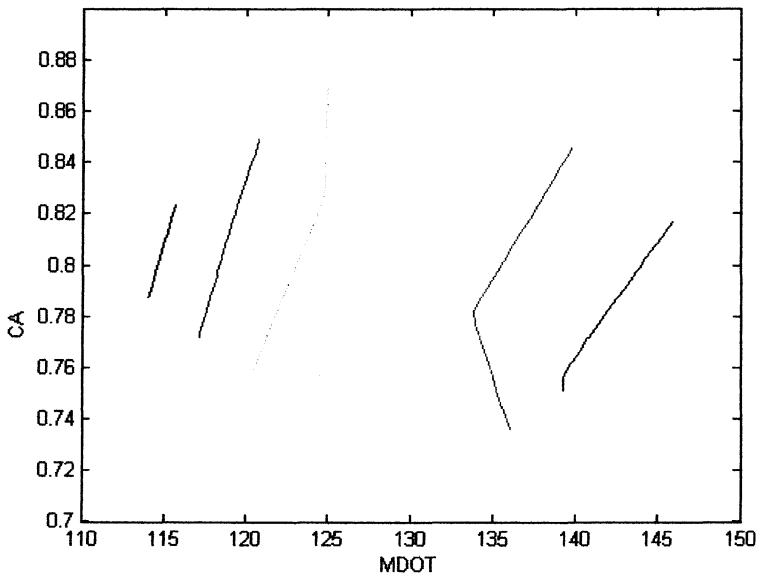

Figure B.8 Contour Plot C_A vs. MDOT

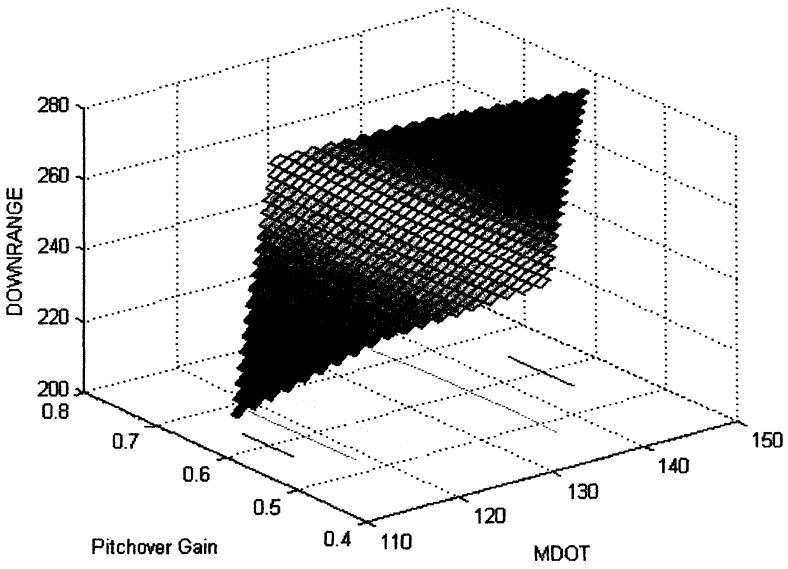

Figure B.9 Response Surface Plot MDOT vs. Pitchover Gain

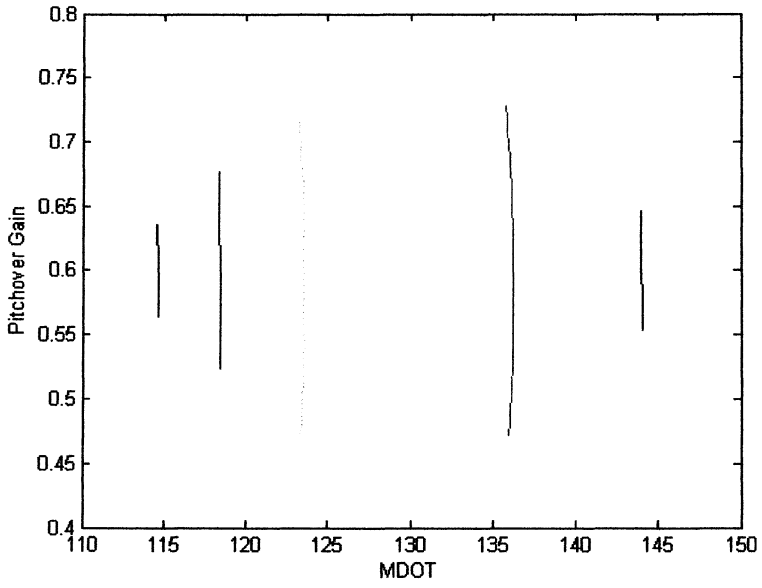

Figure B.10 Contour Plot MDOT vs. Pitchover Gain

APPENDIX C

THREE VARIABLE ANALYSIS WITH PITCHOVER GAIN MATLAB CODES

Response Equation

```
%--------------------------------------------------------------------
%--------------------------------------------------------------------
% Three variable Analysis with Pitchover Gain
% This m-file was created to calculated the coded and natural response
% equations for the V2 simulation.
%--------------------------------------------------------------------
%--------------------------------------------------------------------
% Coded Matrix
% A:MDOT
% B:CA Scale
% C:Pitchover Gain
%--------------------------------------------------------------------
%--------------------------------------------------------------------
I=ones(15,1);
A=[-1;1;-1; 1;-1;1;-1;1;-1.682;1.682;0;0;0;0;0];
B=[-1;-1;1;1;-1;-1;1;1;0;0;-1.682;1.682;0;0;0];
C=[-1;-1;-1;-1;1;1;1;1;0;0;0;0;-1.682;1.682;0];
AA=A.*A;
BB=B.*B;
CC=C.*C;
AB=A.*B;
AC=A.*C;
BC=B.*C;
ABC=A.*B.*C;
X1=[I A B C AB AC BC AA BB CC];
X2=[I A B C AB AC BC AA BB CC ABC];
y=[240.11;271.63;228.16;259.62;240.34;271.85;228.34;259.81;217.8;273.16; ...
   262.06;242.38;251.88;252.32;252.08];
f1=(inv(X1'*X1))*X1'*y
Yprime1=X1*f1
error1=y-Yprime1
%--------------------------------------------------------------------
%Actual Matrix%
% M:Mdot
% N:CA Scale
% O:Pitchover
%--------------------------------------------------------------------
L=ones(15,1);
M=[120;140;120;140;120;140;120;140;113.1820717;146.8179283;130;130;130;
  130;130];
```

```
N=[0.75;0.75;0.85;0.85;0.75;0.75;0.85;0.85;0.8;0.8;0.715910358;0.884089642; ...
0.8;0.8;0.8];
O=[0.5;0.5;0.5;0.5;0.7;0.7;0.7;0.7;0.6;0.6;0.6;0.6;0.432;0.768;0.6];
MM=M.*M;
NN=N.*N;
OO=O.*O;
MN=M.*N;
MO=M.*O;
NO=N.*O;
MNO=M.*N.*O;
J1=[I M N O MN MO NO MM NN OO ];
J2=[I M N O MN MO  NO MM NN OO MNO ];
g=y;
c1=(inv(J1'*J1))*J1'*g;
Jprime1=J1*c1;
errorJ1=g-Jprime1
```

Main Effect Calculations

```
%-------------------------------------------------------------------
% Three Variable Analysis with Pitchover Gain
% main effect equations for V2 simulation RSM
% for downrange responses only
%-------------------------------------------------------------------
n=1;
l= 240.11;
a=271.63;
b=228.16;
ab=259.62;
c=240.34;
ac=271.85;
bc=228.34;
abc=259.81;
aa=217.8;
naa=273.16;
bb=262.06;
nbb=242.38;
cc=251.88;
ncc=252.32;
center=252.08;
 G=1/(4*n);
 m=8*n;
 A=G*((a+ac+abc+ab+aa)-(b+c+bc+l+naa));
 B=G*((b+ab+bc+abc+bb)-(a+c+ac+l+nbb));
 C=G*((c+ac+bc+abc+cc)-(a+b+ab+l+ncc));
 AB=G*((l+ab+c+abc)-(b+a+ac+bc));
 AC=G*((l+b+ac+abc)-(a+ab+c+bc));
  BC=G*((l+a+bc+abc)-(b+ab+c+ac));
  AA=G*(aa-naa)
  BB=G*(bb-nbb);
  CC=G*(cc-ncc);
 ABC=G*((a+b+c+abc)-(l+ab+ac+bc));
 SSA=((A/G)^2)/m;
 SSB=((B/G)^2)/m;
 SSC=((C/G)^2)/m;
 SSAB=((AB/G)^2)/m;
 SSAC=((AC/G)^2)/m;
 SSBC=((BC/G)^2)/m;
 SSABC=((ABC/G)^2)/m;
 R=[SSA;SSB;SSC;SSAB;SSAC;SSBC;SSABC]
```

```
Stationary Point and Ridge Analysis
%-------------------------------------------------------------------
c11=-2.289;
c22=0.09;
c33=0.05;
c12=-0.013;
c13=0;
c23=-0.01;
c=[16.04;-5.94;0.11];
Chat=[c11 c12/2 c13/2;c12/2 c22 c23/2 ;c13/2 c23/2 c33];
Xs_BC=0.5*(inv(Chat))*c
%Xs_BC=[-0.9826;-47.806;-5.408]
if (eig(Chat))>1
   'point is a minimum'
else if (eig(Chat))<1
      'point is a maximum'
   else
      'point is neither'
   end
end
ys_B=252.05+0.5*(Xs_BC)'*c

%-------------------------------------------------------------------
% % Ridge Analysis Iteration
% %-------------------------------------------------------------------
% %-------------------------------------------------------------------
L=0.009;
U=0.10;

lambda=-2.5;
for l=0:0.005:1000;
   lambda_x=lambda-l;
   x_bar=(inv(Chat-lambda_x*eye(3)))*(-0.5*c);
   R=sqrt(x_bar'*x_bar);
   H=R>L;
   S=R<U;
   if and (H,S)
   break
   else
      continue
end
end
R
x_bar
ysB=252.05+0.5*(x_bar)'*c
 yhat=x_bar'*c
```

APPENDIX D

THREE VARIABLE ANALYSIS WITH LAUNCHER ELEVATION ANGLE

MATLAB CODES

Response Equation

```
%--------------------------------------------------------------------------
% Study B
% This m-file was created to calculated the coded and natural response
% equations for the V2 simulation.
%--------------------------------------------------------------------------
%--------------------------------------------------------------------------
% Coded Matrix
% A:Launcher Elevation
% B:MDOT
% C:CASCALE
%--------------------------------------------------------------------------
%--------------------------------------------------------------------------
I=ones(15,1);
A=[-1;1;-1; 1;-1;1;-1;1;-1.682;1.682;0;0;0;0;0];
B=[-1;-1;1;1;-1;-1;1;1;0;0;-1.682;1.682;0;0;0];
C=[-1;-1;-1;-1;1;1;1;1;0;0;0;0;-1.682;1.682;0];
AA=A.*A;
BB=B.*B;
CC=C.*C;
AB=A.*B;
AC=A.*C;
BC=B.*C;
ABC=A.*B.*C;
X1=[I A B C AB AC BC AA BB CC];
X2=[I A B C AB AC BC AA BB CC ABC];
y=[271.92;269.37;302.58;301.08;259.64;257.14;290.03;288.55;283.44; ...
   279.89;248.64;303.23;292.6;272.13;282.33];
f1=(inv(X1'*X1))*X1'*y
Yprime1=X1*f1
error1=y-Yprime1
%--------------------------------------------------------------------------
%--------------------------------------------------------------------------
%--------------------------------------------------------------------------
%Actual Matrix%
% M:Launcher Elevation
% N:MDOT
% O:CASCALE
```

```
%-------------------------------------------------------------------------
%-------------------------------------------------------------------------
L=ones(15,1);
M=[60;80;60;80;60;80;60;80;53.18207169;86.81792831;70;70;70;70;70];
N=[120;120;140;140;120;120;140;140;130;130;113.1820717;146.8179283;130; ...
   130;130];
O=[0.75;0.75;0.75;0.75;0.85;0.85;0.85;0.85;0.8;0.8;0.8;0.8;0.715910358; ...
   0.884089642;0.8];
MM=M.*M;
NN=N.*N;
OO=O.*O;
MN=M.*N;
MO=M.*O;
NO=N.*O;
MNO=M.*N.*O;
J1=[I M N O MN MO NO MM NN OO ];
J2=[I M N O MN MO  NO MM NN OO MNO ];
g=y;
c1=(inv(J1'*J1))*J1'*g;
Jprime1=J1*c1;
errorJ1=g-Jprime1
```

Main Effect Calculations

```
%-------------------------------------------------------------------
% Study B
% main effect equations for V2 simulation RSM
% for downrange responses only
%-------------------------------------------------------------------
n=1;
l= 271.92;
 a=269.37;
 b=302.58;
 ab=301.08;
 c=259.64;
 ac=257.14;
 bc=290.03;
 abc=288.55;
 naa=283.44;
 aa=279.89;
 nbb=248.64;
 bb=303.23;
 cc=292.6;
 ncc=272.13;
 G=1/(4*n);
 m=8*n;
 A=G*((a+ac+abc+ab+aa)-(b+c+bc+l+naa));
 B=G*((b+ab+bc+abc+bb)-(a+c+ac+l+nbb));
 C=G*((c+ac+bc+abc+cc)-(a+b+ab+l+ncc));
 AB=G*((l+ab+c+abc)-(b+a+ac+bc));
 AC=G*((l+b+ac+abc)-(a+ab+c+bc));
  BC=G*((l+a+bc+abc)-(b+ab+c+ac));
 ABC=G*((a+b+c+abc)-(l+ab+ac+bc));
 SSA=((A/G)^2)/m;
 SSB=((B/G)^2)/m;
 SSC=((C/G)^2)/m;
 SSAB=((AB/G)^2)/m;
 SSAC=((AC/G)^2)/m;
 SSBC=((BC/G)^2)/m;
 SSABC=((ABC/G)^2)/m;
 R=[SSA;SSB;SSC;SSAB;SSAC;SSBC;SSABC]
```

Stationary Point and Ridge Analysis

```
%-------------------------------------------------------------------------
% Study B Stationary Point and Ridge Analysis
% Study B coded matrix
%-------------------------------------------------------------------------
c11=-0.1842;
c22=-2.2095;
c33=0.0633;
c12=0.2588;
c13=0.0088;
c23=-0.0712;
c=[-1.0251;15.8139;-6.1516];
Chat=[c11 c12/2 c13/2;c12/2 c22 c23/2 ;c13/2 c23/2 c33];
Xs_BC=0.5*(inv(Chat))*c
%Xs_BC=[-0.9826;-47.806;-5.408]
if (eig(Chat))>1
   'point is a minimum'
else if (eig(Chat))<1
      'point is a maximum'
   else
      'point is neither'
   end
end
ys_B=282.2933+0.5*(Xs_BC)'*c
% %-------------------------------------------------------------------------
% % Study B Ridge Analysis Iteration
% %-------------------------------------------------------------------------
L=0.0009;
U=0.001;
lambda=1.5
for l=0:0.005:1000
   lambda_x=lambda-l;
   x_bar=(inv(Chat-lambda_x*eye(3)))*(-0.5*c)
   R=sqrt(x_bar'*x_bar);
   H=R>L;
   S=R<U;
   if and (H,S)
   break
   else
      continue
end
end
R
ysB=282.2933+0.5*(x_bar)'*c
   yhat=x_bar'*c;
```

REFERENCES

[1] Banks, J., *Handbook of Simulation: Principles, Methodology, Advances, Applications, and Practice*, Wiley, New York, 1998.

[2] Zipfel, P., *Modeling and Simulations of Aerospace Vehicle Dynamics*, AIAA Education Series, AIAA, Virginia, 2000.

[3] Blake, W.B., "Missile DATCOM, A Users Manual", Air Force Research Laboratory, Wright Patterson Air Force Base, Ohio, 1998.

[4] Moore, F. G., *Approximate Methods of Weapon Aerodynamics*, Progress in Astronautics and Aeronautics, AIAA, Virginia, 2000.

[5] Myers, R. H., and Montgomery, D. C., *Response Surface Methodology* 2nd ed., Wiley, New York, 2000.

[6] Anderson, M. J., and Whitcomb, P. J., *RSM Simplified Optimizing Processes Using Response Surface Methods for Design of Experiments*, Productivity Press, New York, 2005.

[7] Box, G., and Draper, N., *Empirical Model-Building and Response Surfaces,* Wiley, New York, 1987.

[8] Brown, D. E., and Schamburg, J. B., "A Modified Response Surface Methodology for Knowledge Discovery with Simulations", *European Journal of Operations Research*, Elsevier Science, Amsterdam, The Netherlands, 2002.

[9] Cioppa, T. M., "Efficient Nearly Orthogonal and Space Filling Experimental Designs for High-Dimensional Complex Models", Doctoral Dissertation, Naval Post Graduate School, Monterey, California, 2002.

[10] Montgomery, D.C., *Design and Analysis of Experiments,* 4th ed., Wiley, New York, 1997.

[11] Starnes, J., Venter, G., and Haftka, R., "Construction of Response Surface Approximations for Design Optimization", *AIAA Journal*, Vol. 36, No. 12, Dec. 1998, pp. 2242-2249.

[12] Harwell, M. R., and Zumbo, B. D., "The Methodology of Methodological Research: Analyzing the Results of Simulations Experiments", Edgeworth Series in Quantitative Behavioral Science, ESQBS-99-2, Prince George, British Columbia, 1999.

[13] Brown, D.E., and Schamburg, J. B., "A Generalized Multiple Response Surface Methodology for Complex Computer Simulation Application", Institute of Electrical and Electronics Engineers, *Winter Simulations Conference,* Washington, D.C., 2004.

[14] Jang, D.H., "A Graphical Method for Evaluating Slope Rotatability in Axial Directions for Second-Order Response Surface Designs", *Journal of Computational Statistics & Data Analysis*, Elsevier Science, Amsterdam, The Netherlands, 2002.

[15] Neufield, M. J., *The Rocket and the Reich*, Harvard University Press, Massachusetts, 1997.

[16] Kennedy, G. P., Vengeance *Weapon 2, The V-2 Guided Missile* Smithsonian Institution Press, Washington, D.C.,1983.

[17] Dungan, T., "V2Rocket.com A-4/V-2 Resource Site", www.v2rocket.com, [retrieved 27 September 2005].

[18] Encyclopedia Astronautica , "V2 Engine",www.astronautix.com/engines, [retrieved 9 September 2006].

[19] Zarchan, P., *Tactical and Strategic Missile Guidance*, 4th ed., Progress in Astronautics and Aeronautics, AIAA, VA, 2002.

[20] Hill, P., and Peterson, C., *Mechanics and Thermodynamics of Propulsion*, 2nd Edition, Addison-Wesley, New York, 1992.

[21] Mason, W.H., "Applied Computational Aerodynamics", Virginia Polytechnic Institute, http://www.aoe.vt.edu/~mason/Mason_f/CAtxtTop.html, [retrieved 20 August 2005].

[22] Stalnaker, J.F., and Robinson, M. A., "Computation of Stability Derivatives of Spinning Missiles Using Unstructured Cartesian Meshes", 20th *AIAA Applied Aerodynamics Conference*, St. Louis, Missouri, 2002.

[23] Robinson, M., Tiger code Version 6.1 Release Notes & Guides, 2006.